13. Geographic Spread and Control of Epidemics

The geographic spread of epidemics is less well understood and much less well studied than the temporal development and control of diseases and epidemics. The usefulness of realistic models for the geotemporal development of epidemics be they infectious disease, drug abuse fads or rumours or misinformation, is clear. The key question is how to include and quantify spatial effects. In this chapter we describe a diffusion model for the geographic spread of a general epidemic which we then apply to a well-known historical epidemic, namely, the ever fascinating mediaeval Black Death of 1347–50. We then discuss practical models for the current rabies epidemic which has been sweeping through continental Europe and is now approaching the north coast of France. These types of models, of course, are not restricted to one disease.

13.1 Simple Model for the Spatial Spread of an Epidemic

We consider here a simpler version of the epidemic model discussed in detail in Chapter 10, Volume I, Section 10.2. We assume the population consists of only two populations, infectives $I(\mathbf{x}, t)$ and susceptibles $S(\mathbf{x}, t)$ which interact. Now, however, I and S are functions of the space variable $\mathbf{x}$ as well as time. We model the spatial dispersal of I and S by simple diffusion and initially consider the infectives and susceptibles to have the same diffusion coefficient D. As before we consider the transition from susceptibles to infectives to be proportional to rSI, where r is a constant parameter. This form means that rS is the number of susceptibles who catch the disease from each infective. The parameter r is a measure of the transmission efficiency of the disease from infectives to susceptibles. We assume that the infectives have a disease-induced mortality rate aI; $1/a$ is the life expectancy of an infective. With these assumptions the basic model mechanism for the development and spatial spread of the disease is then

$$\begin{aligned} \frac{\partial S}{\partial t} &= -rIS + D\nabla^2 S, \\ \frac{\partial I}{\partial t} &= rIS - aI + D\nabla^2 I, \end{aligned} \tag{13.1}$$

where a, r and D are positive constants. These equations are simply (10.1) and (10.2) in Chapter 10, Section 10.2, Volume I with the addition of diffusion terms. The problem we

are now interested in consists of introducing a number of infectives into a uniform population with initial homogeneous susceptible density S_0 and determining the *geo*temporal spread of the disease.

Here we consider only the one-dimensional problem; later we present results of a two-dimensional study. We nondimensionalise the system by writing

$$\begin{aligned} I^* &= \frac{I}{S_0}, \quad S^* = \frac{S}{S_0}, \quad x^* = \left(\frac{rS_0}{D}\right)^{1/2} x, \\ t^* &= rS_0 t, \quad \lambda = \frac{a}{rS_0}, \end{aligned} \tag{13.2}$$

where S_0 is a representative population and the model (13.1) becomes, on dropping the asterisks for notational simplicity,

$$\begin{aligned} \frac{\partial S}{\partial t} &= -IS + \frac{\partial^2 S}{\partial x^2}, \\ \frac{\partial I}{\partial t} &= IS - \lambda I + \frac{\partial^2 I}{\partial x^2}. \end{aligned} \tag{13.3}$$

The three parameters r, a and D in the dimensional model (13.1) have been reduced to only one dimensionless grouping, λ. The basic *reproduction rate* (cf. Chapter 10, Volume I, Section 10.2) of the infection is $1/\lambda$; it has several equivalent meanings. For example, $1/\lambda$ is the number of secondary infections produced by one primary infective in a susceptible population. It is also a measure of the two relevant timescales, namely, that associated with the contagious time of the disease, $1/(rS_0)$, and the life expectancy, $1/a$, of an infective.

The specific problem we investigate here is the spatial spread of an epidemic wave of infectiousness into a uniform population of susceptibles. We want to determine the conditions for the existence of such a travelling wave and, when it exists, its speed of propagation.

We look for travelling wave solutions in the usual way (cf. Chapter 1) by setting

$$I(x,t) = I(z), \quad S(x,t) = S(z), \quad z = x - ct, \tag{13.4}$$

where c is the wavespeed, which we have to determine. This represents a wave of constant shape travelling in the positive x-direction. Substituting these into (13.3) gives the ordinary differential equation system

$$I'' + cI' + I(S - \lambda) = 0, \quad S'' + cS' - IS = 0, \tag{13.5}$$

where the prime denotes differentiation with respect to z. The eigenvalue problem consists of finding the range of values of λ such that a solution exists with positive wavespeed c and nonnegative I and S such that

$$I(-\infty) = I(\infty) = 0, \quad 0 \le S(-\infty) < S(\infty) = 1. \tag{13.6}$$

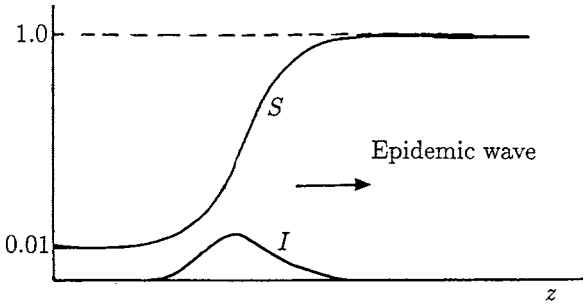

Figure 13.1. Travelling epidemic wave of constant shape, calculated from the partial differential equation system (13.3) with $\lambda = 0.75$ and initial conditions (that is, with compact support) compatible with (13.6). Here a pulse of infectives (I) moves into a population of susceptibles (S) with speed $c = 1$ which in dimensional terms from (13.2) is $(rS_0D)^{1/2}$ which agrees with the analytical wavespeed (13.11) with $\lambda = a/rS_0 = 0.75$.

The conditions on I imply a pulse wave of infectives which propagates into the uninfected population. Figure 13.1 shows such a wave; Figure 13.5 below, which is associated with the spread of a rabies epidemic wave, is another example, although there, only the infectious population I diffuses.

The system (13.5) is a fourth-order phase space system. We can determine the lower bound on allowable wavespeeds c by using the same technique we employed in Chapter 13, Volume I, Section 13.2 in connection with wave solutions of the Fisher–Kolmogoroff equation. Here we linearise the first of (13.5) near the leading edge of the wave where $S \to 1$ and $I \to 0$ to get

$$I'' + cI' + (1 - \lambda)I \approx 0, \tag{13.7}$$

solutions of which are

$$I(z) \propto \exp\left[(-c \pm \{c^2 - 4(1 - \lambda)\}^{1/2})z/2\right]. \tag{13.8}$$

Since we require $I(z) \to 0$ with $I(z) > 0$ this solution cannot oscillate about $I = 0$; otherwise $I(z) < 0$ for some z. So, if a travelling wave solution exists, the wavespeed c and λ must satisfy

$$c \geq 2(1 - \lambda)^{1/2}, \quad \lambda < 1. \tag{13.9}$$

If $\lambda > 1$ no wave solution exists so this is the necessary threshold condition for the propagation of an epidemic wave. From (13.2), in dimensional terms the threshold condition is

$$\lambda = \frac{a}{rS_0} < 1. \tag{13.10}$$

This is the same threshold condition found in Chapter 10, Volume I, Section 10.2 for an epidemic to exist in the spatially homogeneous situation.

With our experience with the Fisher–Kolmogoroff equation we expect such travelling waves computed from the full nonlinear system will, except in exceptional conditions, evolve into a travelling waveform with the minimum wavespeed $c = 2(1-\lambda)^{1/2}$. In dimensional terms, using (13.2), the wave velocity, V say, is then given by

$$V = (rS_0D)^{1/2}c = 2(rS_0D)^{1/2}\left[1 - \frac{a}{rS_0}\right]^{1/2}, \quad \frac{a}{rS_0} < 1. \tag{13.11}$$

The travelling wave solution $S(z)$ cannot have a local maximum, since there $S' = 0$ and the second of (13.5) shows that $S'' = IS > 0$, which implies a local minimum. So $S(z)$ is a monotonic increasing function of z. By linearising the second equation of (13.5) as $z \to \infty$, where $S = 1 - s$, with s small, we have

$$s'' + cs' - I = 0,$$

which, with $I(z)$ from (13.8), shows that

$$S(z) \sim 1 - O\left(\exp[\{-c \pm [c^2 - 4(1-\lambda)]^{1/2}\}z/2]\right)$$

and so, as $z \to \infty$, $S(z) \to 1$ exponentially.

The threshold result (13.10) has some important implications. For example, we see that there is a minimum critical population density $S_c = a/r$ for an epidemic wave to occur. On the other hand for a given population S_0 and mortality rate a, there is a critical transmission coefficient $r_c = a/S_0$ which, if not exceeded, prevents the spread of the infection. With a given transmission coefficient and susceptible population we also get a threshold mortality rate, $a_c = rS_0$, which, if exceeded, prevents an epidemic. So, the more rapidly fatal the disease is, the less chance there is of an epidemic wave moving through a population. All of these have implications for control strategies. The susceptible population can be reduced through vaccination or culling; we discuss this and immunity effects below. For a given mortality and population density S_0, if we can, by isolation, medical intervention and so on, reduce the transmission factor r of the disease, it may be possible to violate condition (13.10) and hence again prevent the spread of the epidemic. Finally with $a/(rS_0) < 1$ as the threshold criterion we note that a sudden influx of susceptible population can raise S_0 above S_c and hence initiate an epidemic.

Here we have considered only a simple two-species epidemic model. We can extend the analysis to a three-species *SIR* system. It becomes, of course, more complicated. In Sections 13.5–13.9 we discuss in some detail such a model for the current European epidemic of rabies.

13.2 Spread of the Black Death in Europe 1347–1350

Historical Aside on the Black Death and Plague in the 20th Century

The fascination with the Black Death, the catastrophic plague pandemic that swept through Europe in the mid-14th century, has not abated with the passage of time. Albert

Camus' *The Plague*, published in 1947, is one example, in a modern context. In the many accounts of the Black Death over the centuries, whether factual or romanticised, a vision has been conjured up of horrific carnage, wild debauchery, unbelievable acts of courage and altruism, and astonishing religious excesses.

The Black Death, principally bubonic plague, was caused by an organism (*Bacillus pestis*) and was transmitted by fleas, mainly from black rats, to man. It was generally fatal. The article by Langer (1964) gives a graphic description and some of the relevant statistics. The historical article by McEvedy (1988) discusses the pandemic's progress and surveys some of the current thinking on the periodic occurrences of bubonic plague. The plague was introduced to Italy in about December 1347, brought there by ship from the East where it had been raging for years. During the next few years it spread up through Europe at approximately 200–400 miles a year. About a quarter to a third of the population died and approximately 80% of those who contracted the disease died within 2–3 days. Figure 13.2 shows the geotemporal spread of the wavefront of the disease.

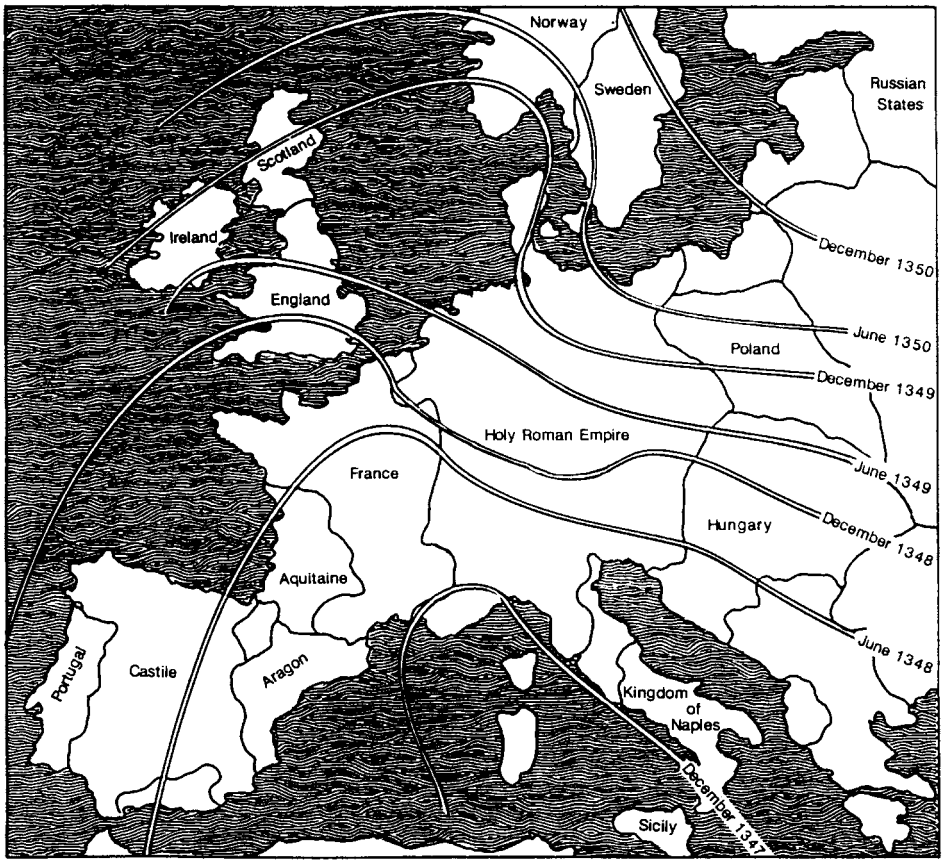

Figure 13.2. Approximate chronological spread of the Black Death in Europe from 1347–1350. (Redrawn from Langer 1964).

After the Black Death had passed, around 1350, a second major outbreak of plague appeared in Germany in 1356. From then on periodic outbreaks seemed to occur every few years although none of them were in the same class as regards severity as the Black Death epidemic of 1347. In Section 13.4 we shall describe an obvious extension to the simple model in this section which takes into account the partial recovery of the population after the passage of an epidemic wave. Including this results in periodic outbreaks, smaller ones, appearing behind the main front: see Figure 13.6 and Figure 13.7. Figures 13.9 and 13.10 in Section 13.5, which consider a three-species model for the spatial spread of a rabies epidemic, exhibit even more dramatic periodic epidemic waves which follow the initial outbreak. There we can estimate the period of the recurring outbreaks analytically.

There was a great variety of reactions to plague in mediaeval Europe and later (just as there is to plague today and the current AIDS epidemic).[1] Groups of penitents, vigorously flagellating their half-naked bodies and preaching the coming of the end of the world, wandered about the countryside; some of the elegant and beautifully carved ivory handles of the flails of the richer flagellants still survive. Cures for the plague abounded during this period. One late 15th century cure, recently discovered in Westfalen-Lippe in northwest Germany, involved the following preparation. The tip of an almost hatched egg was cut off and the brood allowed to run out. The remaining egg yolk was mixed with raw saffron and the egg refilled and resealed with the shell pieces originally removed. The egg was afterwards fried until it turned brown. The recipe then called for the same amount of white mustard, some dill, a crane's beak and theriak (a popular quack medicine of the time). The mixture had to be swallowed by the victim who had to eat nothing more for 7 hours. There is no record of how effective this cure was!

The disease, of which there are three kinds, bubonic, pneumonic and septicemic, is caused by a bacillus carried primarily by fleas which are in turn carried by rats, mice and a host of other animals. Septicemic plague involves the bacilli multiplying extremely rapidly in the victim's blood and is almost invariably fatal (even now), whether treated or not; the victim usually dies very quickly and often suddenly. Septicemic plague often develops from the pneumonic form which is extremely contagious. There are descriptions of plague victims who suddenly sat down and simply keeled over dead. These could well have been septicemic cases who contracted it from the coughs of pneumonic victims. Children at the time of the Great Plague of London from 1664–1666, which peaked in 1665, used to sing the well-known English nursery rhyme

'Ring-a ring o'roses
A pocket full of posies
A-tishoo, A-tishoo
We all fall down.'

[1] John Calvin, the scholar, theologian, unsurpassed killjoy and a man with a monumental ego and self-righteousness was convinced witches acting as agents of the devil brought it to Geneva where he was. He fled, terror stricken, from the epidemic and managed to survive (unfortunately). His baleful influence is still abundantly evident in the Scottish psyche and society even today and has, I am in no doubt, contributed to the massive emigration of Scots over the centuries to escape his depressing, deterministic and unforgiving view of the world.

which is believed to date from that period. Onions and garlic were held to the nose, in 'posies' or the bird-like masks of the physicians, to keep out the bad odours that were thought to be the cause of the disease.

There are considerably more data and information about the Great Plague of London in 1665 than are available about the Black Death. The people's reaction, however, seems not to have been dissimilar—fewer overt extreme penitents perhaps. The diarist Samuel Pepys describes the scene in my own university town of Oxford as one of 'lewd and dissolute behaviour'. Plus ça change. . . ! Daniel Defoe's journal (1722) of the epidemic vividly conjures up a contemporary image and makes fascinating reading: 'It was then indeed, that man withered like the grass and that his brief earthly existence became a fleeting shadow. Contagion was rife in all our streets and so baleful were its effects, that the church-yards were not sufficiently capacious to receive the dead. It seemed for a while as though the brand of an avenging angel had been unloosed in judgment.'

There is a widely held belief that plague more or less ceased to be a problem after the Great Plague of London. This is far from the case, however, as clearly documented in the book by Gregg (1985). The last plague pandemic started in Yunnan in China about 1850 and only finished officially, according to the World Health Organisation, in 1959: more than 13 million deaths have been attributed to it, and it affected most parts of the world. The reported cases (and through ignorance or political expediency the figures must clearly be considered lower bounds) since 1959 makes it clear that plague epidemics are still with us. The thousands who died of it during the Vietnam war, particularly between 1965 and 1975, is a dramatic case to point.

Plague was brought by ship to the Northwest of America around 1900. About 200 deaths were recorded in the three-year San Francisco epidemic which started just after the earthquake in 1906. The article by Risse (1992) is specifically on this San Francisco epidemic. As a result of this epidemic, the western part of the U.S.A., particularly New Mexico, is now one of the two largest residual foci of plague (in mice and voles particularly) in the world—the other is in Russia. The plague bacillus has spread steadily eastwards from the west coast and in 1984 was found among animals in the midwest. The wavefront has moved on average about 35 miles a year. The disease is carried by a large number of native wild animals. Rats are by no means the sole carrier: it has been found in nearly 30 different mammals including, for example, squirrels, chipmunks, coyotes, prairie dogs, mice, voles, domestic pets and bats. The present complacency about the relatively small annual number of plague deaths is hardly justified. If, or rather *when*, plague reaches the east coast of the U.S.A. with its large urban areas, the potential for a serious epidemic will be considerable. New York, for example, has an estimated rat population of one rat per human; and mice—also effective disease carriers — probably number more. The prevailing lack of both concern and knowledge about the plague is dangerous. Plague symptoms are often not recognised or, at best, only belatedly diagnosed. Therefore the victim is free to expose a substantial number of people to the disease, particularly if it is pneumonic plague which is one of the most infectious diseases known.

To return now to our modelling, let us apply our simple epidemic model to the spread of the Black Death. We first have to estimate the relevant parameters, not a simple task with the paucity of hard facts about the social conditions of the time. Noble (1974) used such a model to investigate the spread of the plague and, after a study of

the known facts, suggested approximate values for the parameters, some of which we use.

There were about 85,000,000 people in Europe in 1347 which gives a population density $S_0 \approx 50/\text{mile}^2$. It is particularly difficult to estimate the transmission coefficient r and the diffusion coefficient D. Let us suppose that the spread of news is governed by diffusion with a diffusion coefficient D. The time to cover a distance L miles purely by diffusion is then $O(L^2/D)$ years. Suppose, with the limited communications that existed at the time, that news and minor gossip, say, travelled at approximately 100 miles/year; this gives a value of $D \approx 10^4$ miles^2/year. To transmit the disease the fleas have to jump from rats to humans and humans have to be close enough to infect other humans; this is reflected in the value for r. Noble (1974) estimated r to be 0.4 mile^2/year. He took an average infectious period of two weeks (too long probably), which gives a mortality rate $a \approx 15$/year. These give $\lambda = a/(rS_0) \approx 0.75$. With the wavespeed given by (13.11) in terms of the model parameters, we then get the speed of propagation, V, of the plague as

$$V = 2(rS_0D)^{1/2}\left[1 - \frac{a}{rS_0}\right]^{1/2} \approx 140 \text{ miles/year}.$$

Although this is somewhat lower than the speed of 200 to 400 miles/year, quoted by Langer (1964), it is not an unreasonable comparison in view of the gross estimates used for the unknown, and what are undeterminable, parameters.

Of course, such a model is extremely simple and does not take into account a number of factors, such as the nonuniformity in population density, the stochastic element and so on. Nevertheless it does indicate certain global features of the geographic spread of an epidemic. As we noted in Chapter 10, Section 10.2, Volume I the stochastic model studied by Raggett (1982) for the plague epidemic of 1665 to 1666 in the village of Eyam did not give as good comparison with the data as did the deterministic model. Stochastic elements, however, are more important in spatial models, particularly when the numbers involved are small.

Keeling and Gilligan (2000) have recently proposed an interesting new model for the spatiotemporal spread of the bubonic plague incidence (there are several thousand deaths each year).[2] Plague is a zoonosis (a disease which spreads from animals to humans) and in many areas where it is prevalent rats are clearly implicated. Their model crucially incorporates the rat, as well as human, populations and includes stochasticity. They show that the disease can reside in rat subpopulations thereby letting the disease persist for many years. They discuss both deterministic and stochastic versions of their model and use a cellular automaton model to incorporate spatial stochasticity. From an analysis of their models they obtain, among other things, criteria for the spread in the human population in terms of the rat population. They use data on rodent populations from North America and use current estimates for the parameters.

[2]When I was visiting the Los Alamos National Laboratory in New Mexico in 1985 a 14-year-old boy in the neighbouring village died from getting infected while moving logs from a wood pile in which infected chipmunks had recently died of the disease. He contracted the septicemic form and died within three days.

13.3 Brief History of Rabies: Facts and Myths

Rabies—A Mediaeval View

Rabies is arguably the most horrifying disease; the patient undergoes the most frightening nightmarish experiences before dying in prolonged and terrifying agony. St. Augustine of Hippo included it in a list of disasters he compiled (which included such things as insanity, imprisonment and bankruptcy). In spite of the fact that an effective rabies vaccination is now available, even totally reliable if given soon after being in contact with a rabid animal, the horror of rabies is almost as rampant today as it ever was. If a person reaches the actual rabid stage, that is, displays the clinical symptoms, there is no cure, nor has there ever been a reliably recorded case of a cure. Dr. Patricia Morrison (personal communication, 1992), who has studied historical aspects of the disease, related the following story about the 8th century bishop of Liège, St. Hubert.[3]

A hundred years after Hubert died his corpse was dug up (and reputedly found not to be in a decayed state) and carted off to a poor monastery in the Ardennes. The abbot and monks of the monastery were in dire need of some relic to attract pilgrims, give it some kudos and generally boost morale. Hubert's corpse was just the relic and not surprisingly its arrival was the start of many miraculous cures for the visiting pilgrims. The town, St. Hubert des Ardennes, sprang up around the monastery. In the tourist office, now in the abbot's house of the monastery, you can obtain leaflets about the saint and his conversion. Hubert, a young nobleman, when hunting saw a white stag with a crucifix between its antlers. Christ approached him and he decided to go into the church. Apparently it is complete plagiarism; it was lifted directly from *The Life of St. Eustace*. St. Hubert is the patron saint of hunters. In all the ceremonies that currently take place in the town little is ever mentioned of his role in the rabies story.

In the 11th century a monk wrote that it was customary to take people bitten by a rabid (or supposedly rabid) animal, a dog or wolf generally, to St. Hubert's shrine. The procedure was for the priest to cut the pilgrim's forehead and insert a thread taken from St. Hubert's episcopal stole. The monks later said the stole had been woven by the Virgin Mary and hand delivered by an angel. The connection between the thread ritual (called *la taille*) and rabies is possibly due to the fact that rabies was thought to be caused by worms in a dog's anus or under its tongue. So, the thread from the saint's stole was thought to be a kind of inoculation against rabies. The mediaeval cloak, which never apparently got any smaller, can still be seen in a reliquary in the church, which is enormous and testament to its popularity among pilgrims. Early in the 18th century, during the height of the developing vampire legend (see below), records show that 1956 people were given *la taille*. It still had its followers in the 1920's and I suspect even

[3]The conversation took place in the unlikely venue over dinner in Corpus Christi College, my Oxford College. Dr. Morrison, the art critic of the *Financial Times* (London) subsequently wrote an article for the newspaper ('A saintly 'cure' for rabies,' *Financial Times*, 29–30 August, 1992) which discussed the modelling below, the then current view and the St. Hubert story. I feel it is yet another justification for easy intermingling of the academic disciplines. It greatly helps, of course, if *haute cuisine* is the common fare as it was at 'High Table' where only faculty and their guests can dine.

now.[4] In the church, close to St. Hubert's altar, there is a large iron ring on the wall to which were tied the poor wretches who were writhing, shouting, groaning, barking and convulsing. Occasionally they were 'cured,' in which case St. Hubert had interceded on their behalf. Rabies hysteria, where people thought they had rabies and displayed many of the symptoms of furious rabies, has been well documented. If the poor wretch, who was tied to the ring, after the required nine days wait died then St. Hubert had decided not to intercede. It was very much a win–win situation for St. Hubert and the monastery.

Rabies and the Vampire Legend

Vampires were first mentioned, and widely believed in, during the last quarter of the 17th century. They were thought to be reanimated corpses which rose from their graves, seeking nourishment by sucking the blood of sleeping persons. In the 18th century they were greatly feared, particularly in the Balkans, and were, according to Voltaire 'the sole topic of conversation between 1730 and 1735.' Gómez-Alonso (1998), in an interesting paper on the legend, puts forward a possible explanation for the original belief by suggesting that rabies may have played a role and it is from his work that the following main elements have been taken; his article has a comprehensive list of references both new and old. (Those of a sqeamish bent should perhaps not read the following even though I have omitted many of the even more horrifying descriptions.)

The legend began with a late 17th century report describing the existence of cadavers full of liquid blood, supposedly taken from people and animals. Some villagers alleged to have seen a ghost in the form of a dog, with others a hideous man, that attacked people, seizing them by the throat. Other gory and graphic details are provided in the report. The stories grew. In the village of Medvedja in Serbia in 1731 to 1732 some peasants' deaths were attributed to a vampire. Signs of vampirism were found in 17 exhumed corpses which were pierced with stakes, decapitated and cremated: this was the motivating event for the 'sole topic of conversation' mentioned by Voltaire and picked up by many well-known members of the Enlightenment. Dracula, of literary and film fame, only came into being at the very end of the 19th century.

Vampires were attributed with a wide array of habits, such as leaving their graves to have sexual intercourse as well as to kill innocent victims for their blood. A person could become a vampire if they had been attacked by a vampire or eaten animals that had been killed by one, had died of rabies or plague or even having been a great lover; there were numerous other ways you could become a vampire. Not surprisingly there were also numerous remedies for avoiding becoming a vampire. Two of the visible signs that a corpse was a vampire were prominent genitalia and a body swollen with blood that flowed out of its mouth.

Rabies is a zoononis, that is, a disease that can be transmitted from vertebrates to humans, and in the rabid stage can cause unpredictable violent and aggressive behaviour. Certain diseases of the limbic system can also affect sexual behaviour. Cadavers buried in cold and humid places can often delay decomposition of the corpse by causing the subcutaneous tissue to become waxlike. As to the liquid blood, certain dis-

[4] Dr. Morrison said that when she visited the church and asked the church warden about *la taille* he said that no one believed that nonsense now but did add that he had known of a case and that some people who had been vaccinated after being bitten by what seemed to be a rabid dog had come asking for *la taille*.

eases prolong the liquid stage but when decomposition does set in with dissolution of internal organs, the resulting gases distend various parts of the body such as the genitalia and face and cause the tongue to protrude giving rise to blood frothing from the mouth.

Let us now consider some of the symptoms of human rabies. Most humans develop the 'furious' form of the disease, rather than the paralytic form, and insomnia, uncontrolled agitation, hydrophobia (the former name for the disease), muscular spasms, fear of seeing themselves in a mirror and other extremely ghastly and bizarre manifestations. The spasms can cause the facial muscles to retract the lips showing teeth in a grimace and the emission of unintelligible sounds. There are stories of rabid humans, like rabid dogs, rushing at people and aggressively assaulting (including biting) them. During intermediate quiet times patients drool blood from their mouths. Hypersexuality can also occur with days of permanent erections, frequent intercourse and violent rape attempts (see, for example, Warrell, 1977).

Rabies can be transmitted person-to-person in a variety of ways such as animal (or human) bites, genital mucosae and so on (Warrell, 1977). Numerous theories have been put forward for the legend from simple superstition to schizophrenia. During times of epidemics bodies were sometimes buried in shallow graves and dug up by dogs and wolves, thus giving rise to the idea that vampires rose from their graves. Wandering rabid people pre-19th century could also have given support to the vampire legend with their aggressiveness and hypersexuality. Gómez-Alonso (1998), in his well-documented article, makes a fascinating a highly plausible case for rabies giving rise to the vampire legend. The history of rabies, and attitudes towards it, is fascinating, riveting, often horrifying and sometimes funny.

Rabies: 18th and 19th Century England

Ritvo (1987), in her excellent historical book on animal–human sociology in Victorian England, gives some amazing facts and presents some fascinating insights into the attitudes to rabies in 19th century England. Some of the views and beliefs are hilarious.

In England in the 19th century there were several outbreaks (the numbers were in fact very small) which wreaked havoc and spawned some hilarious laws and views. George Fleming, a distinguished veterinarian, said in his treatise *Rabies and Hydrophobia* that 'there may be some foundation for the supposition that intense sexual excitement may produce rabies . . . .' The interconnection of sex and sin and rabies could be discreetly suggested: the Victorians loved it. The poaching dogs—the 'curs and lurchers'—of the lower classes were considered particlarly prone to rabies.

The geographical range of rabies and its frequency of incidence increased during the 19th century, although the death toll was never very high. For example, 79 people died in 1877, 35 in 1879, 47 in 1875, (which worked out to two rabies deaths per million of population). The average English citizen of the later 19th century was more than 10 times as likely to be murdered as to die of rabies. Ritvo (1987) quotes some hilarious comments at the time such as in the *Kennel Review* which defined hydrophobia (rabies) as 'a peculiar madness that seizes men and impels them to destroy dogs.' A similar view was expressed by the Surgeon General, Charles Alexander Gordon, in his testimony to the House of Lords Committee on rabies.

Remnants of some of the attitudes from a much earlier age, even from mediaeval times, were still evident in the second half of the 20th century and no doubt still exist.

Rabies: Current Situation

Rabies is still a very serious disease that exists with varying degrees of severity in practically all countries of the world except for Britain, Ireland, Sweden, Australia, New Zealand and a few others. The World Health Organisation (WHO 1998) is an excellent source of disease data and it is the source for the latest (1994) global statistics which give some idea of the extant problem with rabies. The estimated number of human cases worldwide is approximately 35,000–45,000 with about 10–20 in Europe, 4–8 in North America, 200–400 in Latin America, 500–5000 in Africa, 35,000–45,000 in Asia and 30,000–40,000 in India. In Bangladesh, for example, in 1994 there were 3000 cases while in the U.S.A. there were 6 with 4 there in each of 1995, 1996 and 1997. France had 1 in 1994 and 3 in each of 1995 and 1996. The number of rabies cases in animals, of course, is very much higher: in the U.S.A. in 1994 there were 8224 confirmed rabies cases while in Bangladesh there were 960 laboratory confirmed cases with 3500 not laboratory confirmed.

Vaccination has been a major control strategy for rabies in parts of Europe. Aubert (1997) describes the status of it in France as a consequence of vaccination (administered via bait in the spring and summer for two years in a row) carried out since 1986. From 1989 to 1996 animal rabies was almost totally eradicated in the regions treated. France created an immunological barrier from the English channel to Switzerland thus stopping the southern progression of the disease. He notes that all cases of canine rabies in the previous 20 years were observed in imported animals, with the last in 1995 and could have been prevented with stricter border controls.

Pastoret (1998) discusses the rabies scene in Belgium and notes that after a period of elimination it appeared again in 1994. Barrat and Aubert (1993) comment on the decline of rabies in France from its peak in 1989 which they partly attribute to the oscillations such as those exhibited by the model.

With such widespread global movement of people and animals it is inevitable that rabies will continue to be introduced into countries hitherto free of the disease. Britain's paranoia about rabies has not been helped with the Channel Tunnel and the fact that bats can carry the disease. Infected bats have been found in parts of Belgium. Teulières and Saliou (1995) noted that although there were no domestic case of rabies from 1970 to 1993, 14 patients contaminated in enzootic areas died from rabies in France. Human vaccination protocol, since 1988, is now based on intramuscular injections, two on day 0 at two different sites with boosters on day 7 and day 21; no failures have been reported. The Center for Disease Control (CDC) in Atlanta recommend booster injections on days 0, 7, 28 and 365 for people in exposed areas; the protection lasts for three years.

The vampire bat is an important reservoir for rabies in, for example, Mexico and Latin America where it has been the origin of rabies outbreaks in cattle. In Asia, Latin America and Africa it is mainly enzootic dog rabies that is the serious problem. Most humans contract the disease through direct bite or scratch from a rabid animal although aerosol transmission in caves with infected bats is also possible. Although rabies is rare in the U.S. when it occurs it is almost always from a bite from an infected bat. Of the 25

cases between 1980 and 1999 all but three contracted it from bats. People bitten by a bat when they are awake will feel the pinch. When asleep, however, the needle-like teeth make practically no wound and may not even be felt; this is probably the likely cause of most of these cases. The Center for Disease Control (CDC) recommends having vaccination (now five shots in the arm over a four-week period) if you wake up and find a bat in your room.

There have been some bizarre and tragic transmissions of the disease including a 14-year-old girl who contracted it from an infected dog that licked her genitals. Human-to-human transmission can also occur: the case of a woman who contracted it from a corneal transplant from a man who was infected (Houff et al. 1979) is particularly ghastly. It was only after both had died from the paralytic form of the disease that the rabies virus was found in their eyes. Corneal transplantation was also implicated in human-to-human transmission in the case of Creutzfeldt–Jakob disease (Duffy et al. 1974) which is considered the human form of BSE—mad-cow disease— contracted from eating beef from infected cows.

13.4 The Spatial Spread of Rabies Among Foxes I: Background and Simple Model

Rabies, as mentioned in the last section, is widespread throughout the world and epidemics are quite common. During the past few hundred years, Europe has been repeatedly subjected to rabies epidemics. It is not known why rabies died out in Europe some 50 or so years before the current epidemic started. The analysis of the models here, however, provides one possible scenario.

The present European epizootic (an epidemic in animals) seems to have started about 1939 in Poland and it has moved steadily westward at a rate of 30–60 km per year. It has been slowed down, only temporarily, by such barriers as rivers, high mountains and autobahns. The red fox is the main carrier and victim of rabies in the current European epidemic. The spread of rabies is like a travelling wave as shown in Figure 13.3.

Rabies, a viral infection of the central nervous system, is transmitted by direct contact, and the dog is the principal transmitter of the disease to man. As mentioned, the incidence of rabies in man, at least in Europe and America, is now rare, with only very few deaths a year, but with considerably more in underdeveloped countries. The effect of rabies on other mammals, domestic and wild, however, is serious. In France, in 1980 alone, 314 cases of rabies in domestic animals were reported and 1280 cases in wild animals. Rabies justifiably gives cause for concern and warrants extensive study and development of control strategies, a subject we discuss later in Section 13.6.

Figure 13.3 shows the advance of the rabies epidemic in France obtained from data from the French *Centre National d'Études sur la Rage* every two years between 1969 and 1977 on the northeastern part of the country. Macdonald (1980) discusses the situation at this time in France in more detail and describes the effects of a vaccination control and what happened when it was stopped. Since this time, however, there has been a concerted effort to control the spread by vaccination through bait and it has been quite successful in several countries in Europe.

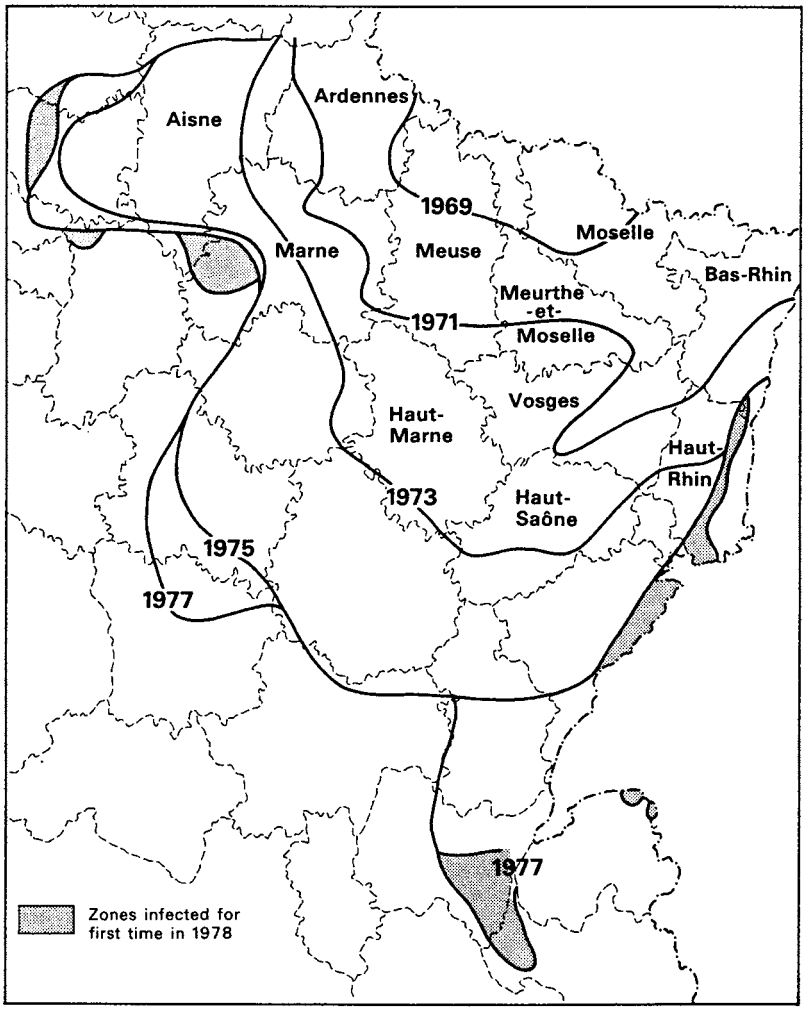

Figure 13.3. Spatial advance of the rabies epizootic in France from 1969 to 1977: note the (heterogeneous) wavelike characteristic of the spatial spread. (Data from *Centre National d'Études sur la Rage*)

A rabies epidemic is also moving rapidly up the east coast of America: the main vector here is the racoon. In this epidemic, the progress was considerably enhanced by the importation into Virginia (by hunting clubs) of infected racoons from Georgia and Florida.

If we refer to Figure 13.1 again, we see that, just as in the spatially uniform epidemic system situation discussed in Chapter 10, Volume I, after the epidemic has passed a proportion of the susceptibles have survived. It would be useful to be able to estimate this survival fraction analytically in a spatial context. This we can do in the following very simple but still illuminating model for the spatial spread of rabies.

Red foxes account for about 70% of the recorded cases in Western Europe. Although Britain has effectively been free from rabies since about 1900, the disease could be reintroduced in the near future through the illegal importation of pets or even by infected bats from the continent. The problem would be particularly serious in Britain because of the high rural and urban density of foxes, dogs and cats. In Bristol, for example, the fox density is of the order of 12 foxes/km^2 as compared with a rural population of 2–4 foxes/km^2. The book on the fox and rabies by Macdonald (1980) provides many of the facts and data for Britain. General data on rabies in Europe is available from the *Centre National d'Etudes sur la Rage* in France. The books edited by Kaplan (1977) and Bacon (1985) are specifically concerned with the population dynamics of rabies and provide biological and ecological background together with some data on the disease.

It is important to understand how the rabies epizootic wavefront progresses into uninfected regions, what control methods might halt it and how the various parameters affect them. The remaining sections of this chapter will be concerned with these specific spatial problems. The material primarily comes from the model of Murray et al. (1986) and, in this section, from the much simpler, but less realistic, model of Källén et al. (1985). The models and control strategies we propose in Sections 13.6 and 13.9 are specifically related to the current European fox epizootic but the type of model is applicable to many other spatially propagating epidemics.

The spatial spread of epidemics is usually a very complex process, and rabies is no exception. In modelling such a complex process we can try to incorporate as many of the facts as possible, which necessarily involves many parameters, estimations of which are difficult to obtain with extant data. An alternative approach is to start with as simple a model as possible but which captures the key elements and for which it is possible to determine estimates for the fewer parameters. There is a trade-off between comprehensiveness and thus complexity, and the difficulty of estimating many parameters and a simpler approach in which parameter values can be reasonably assessed. For the models in this chapter, we have opted for the latter strategy. In spite of their simplicity, they nevertheless pose highly relevant practical questions and give estimates for various characteristics of importance in the spatial spread of diseases. Although in this section we describe and analyse a particularly simple model, it is one for which we can obtain useful analytical results.

Although many animals are involved, a basic, and reasonable, assumption is that the ecology of foxes, the principal vectors, determines the dynamics of the spread of rabies. We further assume that the spatial spread of the epizootic is due primarily to the random erratic migration of rabid foxes. Uninfected foxes do not seem to wander far from their territory (Macdonald 1980). We divide the fox population into two groups—susceptible and rabid. Although the resulting model captures certain aspects of the spatial spread of the epizootic front, it leaves out a basic feature of rabies, namely, the long incubation period of between 12 and 150 days from the time of an infected bite to the onset of the clinical infectious stage. We include this in the more realistic model presented in Section 13.5.

To control, and ideally prevent, the spread of the disease, it is important to have some understanding of how rabies spreads so as to assess the effects of possible control strategies. It is with this in mind that we first study a particularly simple modified version

of the epidemic model system (13.1), which captures some of the key elements in the spread of rabies in the fox population. We shall then use it to derive some estimates of essential facts about the epizootic wave.

We consider the foxes to be divided into two groups, infectives I, and susceptibles S; the infectives consist of rabid foxes and those in the incubation stage. The principal assumptions are: (i) The rabies virus, contained in the saliva of the rabid fox, is transmitted from the infected fox to the susceptible fox. Foxes become infected at an average rate per head, rI, where r is the transmission coefficient which measures the rate of contact between the two groups. (ii) Rabies is invariably fatal and foxes die at a per capita rate a; that is, the life expectancy of an infected fox is $1/a$. (iii) Foxes are territorial and divide the countryside into non-overlapping ranges. (iv) The rabies virus enters the central nervous system and induces behavioral changes in the fox. If the virus enters the spinal cord it induces paralysis whereas if it enters the limbic system it induces transient aggression during which it loses its sense of territory and the fox wanders about in a more or less random way. So, we assume that it is only the infectives which disperse with diffusion coefficient $D\text{km}^2/\text{year}$. With these assumptions our model is then (13.1) except that the susceptible foxes do not disperse. We exclude here the migration of cubs seeking their own territory. When they do move they try to stay as close to their original territory as possible. The model system in one dimension is then

$$\begin{aligned} \frac{\partial S}{\partial t} &= -rIS, \\ \frac{\partial I}{\partial t} &= rIS - aI + D\frac{\partial^2 I}{\partial x^2}. \end{aligned} \tag{13.12}$$

From the analysis in the last section we expect this system to possess travelling wave solutions, whose speed of propagation depends intimately on the parameter values. The realistic estimation of these few parameters is important but still not easy.

Using the nondimensionalisation (13.2), the system (13.12) becomes (cf. (13.3))

$$\begin{aligned} \frac{\partial S}{\partial t} &= -IS, \\ \frac{\partial I}{\partial t} &= IS - \lambda I + \frac{\partial^2 I}{\partial x^2}, \end{aligned} \tag{13.13}$$

where now S, I, x and t are dimensionless, and, as in the last section, $\lambda = a/rS_0$ is a measure of the mortality rate as compared with the contact rate. As before the contact rate is crucial and is not known with any confidence. We expect the threshold value to be again $\lambda = 1$ but we now verify this (see also Exercise 2).

Travelling wavefront solutions of (13.13) are of the form

$$S(x,t) = S(z), \quad I(x,t) = I(z), \quad z = x - ct, \tag{13.14}$$

where c is the wavespeed and we look for solutions satisfying the boundary conditions

$$S(\infty) = 1, \quad S'(-\infty) = 0, \quad I(\infty) = I(-\infty) = 0. \tag{13.15}$$

Refer back to Figure 13.1 for the type of wave anticipated. Note that it is the *derivative* of $S(z)$ which tends to zero as $z \to -\infty$ since we anticipate a residual number, as yet undetermined, of susceptible foxes to survive the epidemic. With (13.14) the system (13.13) becomes

$$\begin{aligned} cS' &= IS, \\ I'' + cI' + I(S - \lambda) &= 0. \end{aligned} \tag{13.16}$$

Linearising about $I = 0$ and $S = 1$ exactly as we did in the last section and requiring I to be always nonnegative, we find that this requires $\lambda < 1$, in which case the wavespeed

$$c \geq 2(1 - \lambda)^{1/2}, \quad \lambda < 1. \tag{13.17}$$

With this specific model we are able to take the analysis further and find the actual fraction of susceptibles which survives the epidemic. From the first of (13.16), $I = cS'/S$, which on substituting into the second equation gives

$$I'' + cI' + \frac{cS'(S - \lambda)}{S} = 0.$$

Integration gives

$$I' + cI + cS - c\lambda \ln S = \text{constant}.$$

Using the boundary conditions as $z \to \infty$ from (13.15), where $S = 1$, $I = 0$ and with $I' = 0$, we determine the constant to be c. If we now let $z \to -\infty$, again using (13.15) with $I = I' = 0$, we get the following transcendental equation for the surviving susceptible population, σ say, after the passage of the epizootic wavefront,

$$\sigma - \lambda \ln \sigma = 1, \quad \lambda < 1, \quad \sigma = S(-\infty), \tag{13.18}$$

which is independent of c. Writing this in the form

$$\frac{\sigma - 1}{\ln \sigma} = \lambda < 1 \Rightarrow 0 < \sigma < \lambda < 1. \tag{13.19}$$

From (13.19), with $\lambda = 0.4$, $\sigma = 0.1$ for example, whereas with $\lambda = 0.7$, $\sigma = 0.5$. λ is a measure of the severity of the epidemic. The smaller λ the fewer susceptibles survive; in other words, the worse the epidemic. Figure 13.4 illustrates the surviving susceptible fraction σ as a function of λ obtained from (13.18); the curve was obtained by plotting λ as a function of σ.

The critical bifurcation value for λ is $\lambda = 1$, which in dimensional terms, from (13.2), means $a/(rS_0) = 1$. If $\lambda > 1$ no epidemic wave can propagate. This is to be expected since if $a > rS_0$ it means the mortality rate is greater than the rate of recruitment of new infectives. As before this bifurcation result says that given r and a,

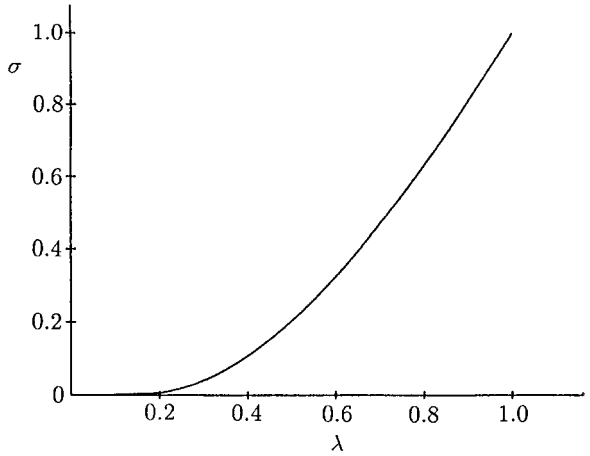

Figure 13.4. The fraction, σ, of the original susceptible fox density which survive, after the passage of the epidemic wave, as a function of the epidemic severity: here, in terms of the original dimensional variables, $\sigma = S(-\infty)/S_0$ and $\lambda = a/(rS_0)$.

there is a critical minimum fox density $S_c = a/r$ below which rabies cannot persist in the population and any infectives introduced will not cause an epidemic.

When rabies does persist, that is, $\lambda < 1$, the computed speed of propagation of the epidemic wave is the minimum of the allowable speeds, namely, $c = 2(1-\lambda)^{1/2}$, which in dimensional terms from (13.17) and (13.2) is

$$c = 2[D(rS_0 - a)]^{1/2}. \tag{13.20}$$

Figure 13.5 shows an example of the computed travelling front solutions for S and I, from (13.13), for $\lambda = 0.5$. From Figure 13.4 with $\lambda = 0.5$, the surviving fraction of susceptibles $\sigma \approx 0.2$.

Let us now compare the qualitative form of the susceptible fox population in the epidemic in Figure 13.5 with that obtained from data from continental Europe as illus-

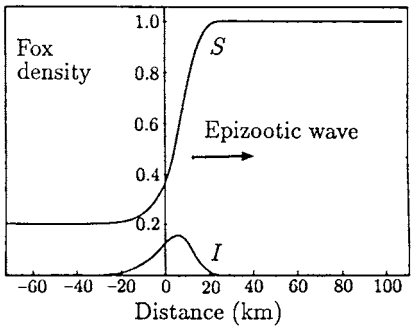

Figure 13.5. Dimensionless epidemic wavefront solution for the susceptible (S) and infected (I) fox populations computed from (13.13): here $\lambda = 0.5$. The wavespeed is $c = \sqrt{2}$. Note the qualitative similarity with Figure 13.1.

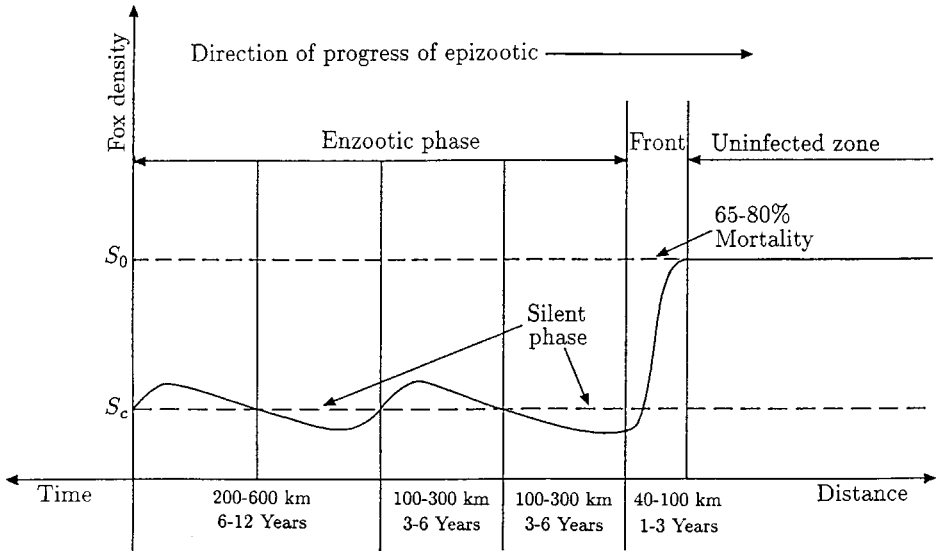

Figure 13.6. Fluctuations in the susceptible fox population density as a function of the passage of the rabies epizootic obtained from data from *Centre National d'Etudes sur la Rage* 1977. In dimensional terms, S_0 is the uninfected susceptible population ahead of the epidemic wave. Note the periodic, but decreasing, fluctuations in S, which follow the main wavefront, as S tends to its steady state. (Redrawn from Macdonald 1980).

trated in Figure 13.6. There is a clear schematic difference in the behaviour behind the front in the two figures. The model (13.13) is only intended to cover the passage of an epidemic front. Clearly after the passage of the wavefront the susceptible population will start to increase again since the foxes find themselves in an environment which admits a larger carrying capacity. In other words, the timescale of the model (13.13) is considerably shorter than that associated with the oscillations in Figure 13.6. To include in our model the situation which obtains after the front has passed we must include a term for the fox reproduction. If we model this by a simple logistic growth, the equation for the susceptibles in place of the first of (13.13) becomes

$$\frac{\partial S}{\partial t} = -rIS + BS\left(1 - \frac{S}{S_0}\right), \tag{13.21}$$

where B is the linear growth rate. With the same nondimensionalisation (13.2) as before, the model now becomes

$$\begin{aligned} \frac{\partial S}{\partial t} &= -IS + bS(1 - S), \\ \frac{\partial I}{\partial t} &= I(S - \lambda) + \frac{\partial^2 I}{\partial x^2}, \end{aligned} \tag{13.22}$$

where $b = B/rS_0$, that is, the ratio of linear birth rate to the basic rate of infection per infective. Figure 13.7 shows an example of the resulting epidemic wave of susceptibles

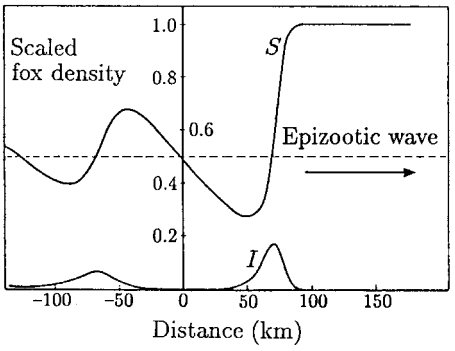

Figure 13.7. Travelling epidemic wave solution for the susceptible (S) and infective (I) foxes from (13.22) when logistic growth is taken into account in the susceptible fox population: parameter values $b = 0.05$, $\lambda = 0.5$. Note the qualitative similarity with the data illustrated in Figure 13.6. The initial front is succeeded by recurring, but smaller, outbreaks of the disease. (After Källén et al. 1985).

and infectives, obtained by numerically solving (13.22); there is now good qualitative comparison between the results from this model and the data recorded in Figure 13.6. The oscillations are decaying and eventually $S \to \lambda$ and $I \to b(1-\lambda)$, the steady state solutions of (13.22), far behind the front.

Although the wavelength of the quasi-periodic outbreaks in both time and space are given by the numerical solutions, we can obtain some useful analytical results even for this more complex model (13.22). Let us start with the dimensional version of (13.22), namely,

$$\begin{aligned} \frac{\partial S}{\partial t} &= -rSI + BS\left(1 - \frac{S}{S_0}\right), \\ \frac{\partial I}{\partial t} &= rSI - aI + D\frac{\partial^2 I}{\partial x^2}. \end{aligned} \tag{13.23}$$

If we now introduce the nondimensional quantities

$$\begin{aligned} &U = \frac{S}{S_0}, \quad V = \frac{rI}{BS_0}, \quad t^* = BT, \quad x^* = \left(\frac{B}{D}\right)^{1/2} x, \\ &\lambda = \frac{a}{rS_0}, \quad \alpha = \frac{rS_0}{B}, \end{aligned} \tag{13.24}$$

the dimensionless model becomes, on omitting the asterisks for notational simplicity,

$$\begin{aligned} U_t &= U(1 - U - V), \\ V_t &= \alpha V(U - \lambda) + V_{xx}. \end{aligned} \tag{13.25}$$

These equations are the same as equations (1.3) in Chapter 1, but without prey diffusion and with α and λ here in place of a and b there, and is the system we studied in detail in Section 1.2. The steady state solutions of (13.25) are $(0, 0)$, $(1, 0)$ and $(\lambda, 1-\lambda)$ with the latter existing in the positive quadrant only if $\lambda < 1$. If we look for travelling wave solutions in the usual way (cf. equations (1.5)), the analysis of the three-dimensional

phase space (U, V, W), where $W = V'$, is given in Section 1.2. There we showed that with $\lambda < 1$ a travelling wave solution exists which joins the steady states $(1, 0)$ and $(\lambda, 1 - \lambda)$. We also showed that a threshold $\alpha = \alpha^*$ exists such that if $\alpha > \alpha^*$ the approach to the steady state $(\lambda, 1 - \lambda)$ is oscillatory, whereas if $\alpha < \alpha^*$ it is monotonic (cf. Figure 1.3). The computed solution in Figure 13.7 is an example with $\alpha > \alpha^*$.

Let us now return to the observation in Section 13.2 about the subsequent outbreaks of plague which followed the initial Black Death epidemic. If we modify the susceptible equation in the model (13.1) to take into account the recovery of the population we again get subsequent periodic outbreaks of the disease following the initial epidemic similar to those shown in Figures 13.6 and 13.7. This is just a bit too facile an explanation since it was the interaction of populations which governed the Black Death, people, fleas, rats and so on. In spite of the simplicity of the model discussed here the results qualitatively capture some of the major phenomena observed. As with so many of the models we have discussed, even such a simple approach can elicit relevant questions.

13.5 The Spatial Spread of Rabies Among Foxes II: Three-Species (*SIR*) Model

To be of practical use in developing control strategies to contain the spatial spread of an epidemic, we have to consider more realistic and hence more complex models, which allow for quantitative comparison with known data and let us make practical predictions with more confidence. The model in the last section, although capturing certain aspects of the spread of an epizootic front, is rather too primitive for quantitative purposes. One of the major exclusions from the previous model is the long incubation period, which, as mentioned above, can be from 12 to 150 days, before the fox becomes rabid. In this section we consider a more realistic model which takes this, among other things, into account. With it we can obtain quantitative estimates for various times and distances of epidemiological and public health significance.

In this section we consider a three-species model where again the rabid foxes are considered the main cause of the spatial spread. The data on the movement of rabid foxes in the wild, although rather scant, is not zero; some of it will be used later when we estimate the crucial diffusion coefficient for rabid foxes.

The model we develop is still comparatively simple, but, even so, some of the parameters are difficult to estimate from the available data. Such parameter estimates will be required in any realistic models, so it is important to learn more about fox ecology and the impact of rabies on fox behaviour in order to improve on the estimation of the more critical parameters.

The model, analysis and results we give here are based on the work of Murray et al. (1986) who give further details and results. It extends the work of Anderson et al. (1981) (who considered only the time-dependent situation) by including spatial effects, specifically the crucial spatial dispersal of rabid foxes and later in Section 13.9 the dispersal of all foxes.

We consider a three-species *SIR* model in which we divide the fox population into susceptible foxes, S, infected, but noninfectious, foxes, I, and infectious, rabid foxes, R.

The need for at least three species is primarily based on the long incubation period of from 12 to 150 days (and in some cases longer) that the rabies virus undergoes in the infected animal, during which time the animal appears to behave normally and does not seem to transmit the disease, and on the relatively short period (1 to 10 days) of clinical disease which follows.

The basic model assumptions are closely linked to those in the last section (we use a slightly different notation) but we reiterate them here for convenience. The assumptions are:

(i) The dynamics of the fox population in the absence of rabies can be approximated by the simple logistic form

$$\frac{dS}{dt} = (a-b)S\left(1-\frac{S}{K}\right),$$

where a is the linear birth rate, b is the intrinsic death rate and K is the environmental carrying capacity. The parameters a, b and K may vary according to the habitat but at this stage we take them to be constants. Later, when we present the numerical results for the English 'experiment,' we shall consider K to vary, as it does in a major way in England.

(ii) Rabies is transmitted from rabid to susceptible fox by direct contact between foxes, usually by biting. Susceptible foxes become infected at an average per capita rate βR, which is proportional to the number of rabid foxes present, where the transmission coefficient β, taken to be constant, measures the rate of contact between the two species.

(iii) Infected foxes become infectious (rabid) at an average per capita rate, σ, where $1/\sigma$ is the average incubation time.

(iv) Rabies is invariably fatal, with rabid foxes dying at an average per capita rate α: $1/\alpha$ is the average duration of clinical disease.

(v) Rabid and infected foxes continue to put pressure on the environment, and die of causes other than rabies, but they have a negligible number of healthy offspring. These effects are small but are included for completeness.

To take into account the spatial effects we make the following further assumptions.

(vi) Foxes are territorial, and divide the countryside up into nonoverlapping ranges.

(vii) Rabies acts on the central nervous system with about half of infected foxes having the so-called 'furious rabies', and exhibit the ferocious symptoms typically associated with the disease, while with the rest the virus affects the spinal cord and causes paralysis. Foxes with furious rabies may become aggressive and confused, losing their sense of direction and territorial behaviour, and wandering randomly. It is these we consider the main cause of the spatial spread of the disease.

These assumptions suggest the following model for the spatial and temporal evolution of the rabies epizootic.

$$\begin{aligned}
\frac{\partial S}{\partial T} &= aS - bS - \frac{(a-b)NS}{K} - \beta RS, \\
\frac{\partial I}{\partial T} &= -bI - \frac{(a-b)NI}{K} + \beta RS - \sigma I, \\
\frac{\partial R}{\partial T} &= -bR - \frac{(a-b)NR}{K} + \sigma I - \alpha R + D\frac{\partial^2 R}{\partial X^2},
\end{aligned} \tag{13.26}$$

where the total population

$$N = S + I + R. \tag{13.27}$$

We have written the equations in this form to highlight what each term means. The only source term comes from the birth of susceptible foxes. All die naturally; the life expectancy is $1/b$ years. The term $(a-b)N/K$ in each equation represents the depletion of the food supply by all foxes. The transition from susceptible to infectious foxes is accounted for by the βRS term and from the infected to the infectious group by σI. Rabid foxes also die from rabies and thus are represented by the αR term; the life expectancy of a rabid fox is $1/\alpha$. Rabid foxes also diffuse with diffusion coefficient D. Typical parameter values, except for the crucially important D, are given in Table 13.1. If, in the absence of any spatial effects, we add equations (13.26) we get

$$\frac{dN}{dt} = aS - bN - \frac{(a-b)N^2}{K} - \alpha R, \tag{13.28}$$

which is the equivalent logistic form for the total population.

We have written the equations in one-dimensional form but we shall use the full two-dimensional form when we apply the model to the spread of the disease from a hypothetical outbreak in England, which we discuss later.

This model neglects the spatial dispersal of rabies by young itinerant foxes, who may get bitten while in search of a territory and carry rabies with them before they become rabid. There is some justification for this since rabies is much less common in the young than in adults (Artois and Aubert 1982, Macdonald 1980).

Table 13.1. Parameter values for rabies among foxes (from Anderson et al. 1981).

Parameter	Symbol	Value
Average birth rate	a	1 fox year^{-1}
Average intrinsic death rate	b	0.5 fox year^{-1}
Average duration of clinical disease	$1/\alpha$	5 days
Average incubation time	$1/\sigma$	28 days
Critical carrying capacity	K_T	1 fox km^{-2}
Disease transmission coefficient	β	80 km^2 year^{-1}
Carrying capacity	K	0.25–4.0 foxes km^{-2}

The spatially homogeneous steady state solutions of (13.26), other than the zero steady state, are given, after some algebra, by

$$\begin{aligned} S_0 &= \beta^{-1}[\sigma\beta K - a(a-b)]^{-2}\{[(\alpha+b)\beta K \\ &\quad + (a-b)(\alpha+a)][\sigma\beta K(\sigma+b) + \alpha(a-b)(\sigma+a)]\}, \\ I_0 &= [\sigma\beta K - a(a-b)]^{-1}[(\alpha+b)\beta K + (a-b)(\alpha+a)]R_0, \\ R_0 &= \{\beta[\sigma\beta K - a(a-b)]\}^{-1}(a-b)[\sigma\beta K - (\sigma+a)(\alpha+a)]. \end{aligned} \tag{13.29}$$

In the spatially uniform situation ($D = 0$), when rabies is introduced into a stable population of healthy foxes three possible behaviours are possible. Which behaviour occurs depends on the size of K relative to the critical carrying capacity K_T which is given by the condition for a nonzero value for the steady state R_0 in the last equation, namely,

$$K_T = \frac{(\sigma+a)(\alpha+a)}{\sigma\beta}. \tag{13.30}$$

If $K < K_T$, the epidemic threshold value of the carrying capacity, rabies eventually disappears ($R \to 0, I \to 0$), and the population returns to its initial value $S = K$. On the other hand, if K is larger than K_T, then the population oscillates about the steady state. From a standard linear stability analysis of the steady state (S_0, I_0, R_0), the equivalent of which we do below for $K > K_T$, it can be shown (after some algebra) that if K is not too much bigger than K_T the steady state is stable and perturbations die out in an oscillatory way. On the other hand, if K is sufficiently larger than K_T limit cycle solutions exist. There are thus 2 bifurcation values for K, namely, K_T and the critical K between a limit cycle oscillation and a stable steady state.

From the epidemiological evidence, rabies seems to die out if the carrying capacity is somewhere between 0.2 and 1.0 foxes/km^2 (WHO Report 1973, Macdonald 1980, Steck and Wandeler 1980, Anderson et al. 1981, Boegel et al. 1981). The parameter β, which is a measure of the contact rate between rabid and healthy foxes, cannot be estimated directly given the difficulties involved in observing these contacts. Anderson et al. (1981) used the expression (13.30) as an indirect way to estimate β since we have estimates for K_T and all the other parameters except β. Parameter estimation is always an important aspect of any realistic modelling. Murray et al. (1986) discuss in some detail how they affect the spatial spread of rabies: the model is quite robust to variations in many of the parameters within a band around the estimates used. Another method for getting parameter information with observational limitations is given by Bentil and Murray (1991).

With $K > K_T$ the parameter choices listed in Table 13.1, give 3–5 year periods for the oscillations and 0 to 4% *equilibrium persistence*, p, of rabies, where p is defined by

$$p = \frac{R_0 + I_0}{S_0 + I_0 + R_0}. \tag{13.31}$$

These figures are in agreement with the available epidemiological evidence (Toma and Andral 1977, Macdonald 1980, Steck and Wandeler 1980, Jackson and Schneider 1984).

Travelling Epizootic Wavefronts and Their Speed of Propagation

We introduce nondimensional quantities by setting

$$\begin{aligned} &s = \frac{S}{K}, \quad q = \frac{I}{K}, \quad r = \frac{R}{K}, \quad n = \frac{N}{K}, \\ &\varepsilon = \frac{a-b}{\beta K}, \quad \delta = \frac{b}{\beta K}, \quad \mu = \frac{\sigma}{\beta K}, \quad d = \frac{\alpha+b}{\beta K}, \\ &x = \left(\frac{\beta K}{D}\right)^{1/2} X, \quad t = \beta K T, \end{aligned} \tag{13.32}$$

with which the model equations (13.26) with (13.27) become

$$\begin{aligned} \frac{\partial s}{\partial t} &= \varepsilon(1-n)s - rs, \\ \frac{\partial q}{\partial t} &= rs - (\mu + \delta + \varepsilon n)q, \\ \frac{\partial r}{\partial t} &= \mu q - (d + \varepsilon n)r + \frac{\partial^2 r}{\partial x^2}, \\ n &= s + q + r, \end{aligned} \tag{13.33}$$

which have a positive uniform steady state solution (s_0, q_0, r_0) given by equations (13.29) on dividing (S_0, I_0, R_0) by K. The condition (13.30) for an epidemic to occur, namely, $K > K_T$, is then

$$0 < d < \left[1 + \frac{\delta + \varepsilon}{\mu}\right]^{-1} - \varepsilon. \tag{13.34}$$

The system (13.33) now depends on only 4 dimensionless parameters ε, δ, μ and d as compared with the original dimensional system's 7 parameters. Values for these dimensionless parameters are obtained from the parameter estimates of a, b, α, σ, K and β in Table 13.1. If we choose a representative carrying capacity of $K = 2$ foxes/km^2 we get $\varepsilon = \delta = 0.003$, $\mu = 0.08$ and $d = 0.46$. The fact that ε and δ are relatively small numbers compared to any of 1, μ, δ and $1 - d$ can be used to simplify the analysis of the model system (13.33) and lets us derive useful *analytical* results; see below and Murray et al. (1986).

It is perhaps appropriate here to reiterate yet again the major benefit of nondimensionalisation, namely, that the parameter groupings show equivalent effects of variations in actual field parameters. For example, with ε and δ small this means that, during the epidemic, the infectious rate is relatively very much larger than the birth and death rates from causes other than rabies.

Let us now look for epizootic wave solutions to the system (13.33), which travel at a constant velocity v into an undisturbed, rabies-free region. (For algebraic simplicity we use a different notation from what we have used earlier in this chapter.) So, we look for solutions s, q and r as functions of the single variable $\xi = x + vt$, which thus satisfy

$$\begin{aligned} vs' &= \varepsilon(1-n)s - rs, \\ vq' &= rs - (\mu + \delta + \varepsilon n)q, \\ vr' &= \mu q - (d + \varepsilon n)r + r'', \\ n &= s + q + r, \end{aligned} \tag{13.35}$$

where prime denotes differentiation with respect to ξ and where $s \to 1, q \to 0, r \to 0$ as $\xi \to -\infty$, that is, far ahead of the wavefront. As usual, of course, we are interested only in nonnegative solutions. In the following we use the fact that $\varepsilon \ll 1$ and $\delta \ll 1$.

The system (13.35) has three possible steady state solutions for (s, q, r) in the positive quadrant, namely, $(1, 0, 0)$, $(0, 0, 0)$ and (s_0, q_0, r_0), where s_0, q_0 and r_0 are given by (13.29) on dividing by K. Since ε and δ are small, to first-order in ε and δ,

$$s_0 = d + \left[\varepsilon + \frac{\varepsilon d + \delta}{\mu}\right] d, \quad q_0 = \frac{\varepsilon d(1-d)}{\mu}, \quad r_0 = \varepsilon(1-d). \tag{13.36}$$

From the full expressions for (s_0, q_0, r_0) all of s_0, q_0 and r_0 are nonnegative only if the threshold condition (13.34) is satisfied.

A travelling wave solution to (13.35), with the required properties, is a trajectory in the 4-dimensional phase space of (13.35), which goes from the equilibrium at $s = 1$, $q = r = 0$ to one of the other two equilibrium points, $(0, 0, 0)$ or (s_0, q_0, r_0). We do not carry out all the algebra since the procedure is the customary one used throughout both Volume I and II; we just briefly describe the various steps and leave the details to be worked out as an exercise.

We write (13.35) as a 4-dimensional first-order system in (s, q, r, r') and first linearise about the critical point $(s, q, r, r') = (1, 0, 0, 0)$. In the usual way, this gives a linear system whose solutions are linear combinations of the eigensolutions $\mathbf{x}_i \exp(\lambda_i \xi)$, where $\mathbf{x}_i$ and λ_i are the four eigenvectors and eigenvalues of the stability matrix. We can thus determine the solution behaviour near the critical point by looking at all possible linear combinations of the eigensolutions. If $\operatorname{Re}\lambda_i < 0$, then $\mathbf{x}_i \exp(\lambda_i \xi) \to 0$ as $\xi \to \infty$ and the trajectory approaches the critical point, while if $\operatorname{Re}\lambda_i > 0$ the trajectory comes out of the critical point. Trajectories leaving the critical point thus correspond to linear combinations of those eigensolutions with $\operatorname{Re}\lambda_i > 0$. If an eigenvalue is complex, then its eigensolution is oscillatory. After some algebra we find that the four eigenvalues for the linear system near $(1, 0, 0, 0)$ are $\lambda = -\varepsilon/v < 0$ and the roots of the cubic

$$\begin{aligned} f(\lambda) = \lambda^3 + \left(\frac{\mu + \delta + \varepsilon}{v} - v\right)\lambda^2 - (d + \mu + \delta + 2\varepsilon)\lambda \\ + \frac{\mu(1 - d - \varepsilon) - (\delta + \varepsilon)(d + \varepsilon)}{v}. \end{aligned} \tag{13.37}$$

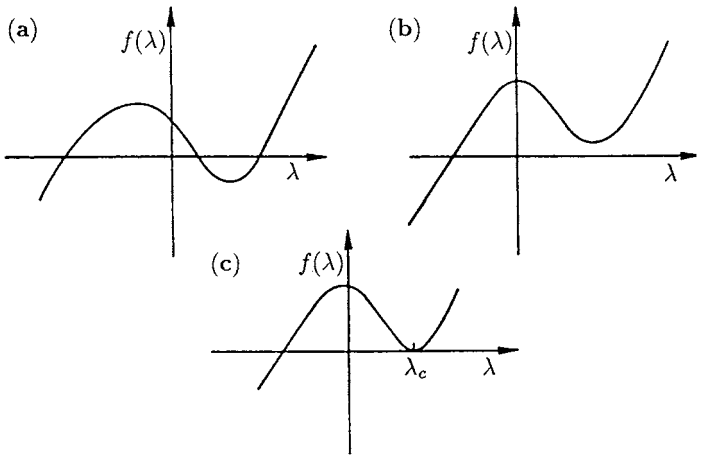

Figure 13.8. The eigenfunction cubic $f(\lambda)$ in (13.37), the zeros of which are eigenvalues of the linearised system about (1, 0, 0). The solutions have either two positive roots as in (**a**), two complex roots with $\mathrm{Re}\,\lambda > 0$ as in (**b**), or a double real root at λ_c as in (**c**).

Note that $f(\lambda) \to \infty$ as $\lambda \to \infty$ and $f(\lambda) \to -\infty$ as $\lambda \to -\infty$. Further, if (13.36) holds, then $f(0) > 0$ and f has a negative slope at $\lambda = 0$. Depending on the values of the various parameters, $f(\lambda)$ can look like any of the forms illustrated in Figure 13.8.

With all the parameters fixed, as the velocity v is varied $f(\lambda)$ sequentially looks like each of these shapes. Thus, as long as the threshold condition (13.34) holds, f has one negative real root and, depending on the value of the velocity of the wave, it has either two positive real roots, or two complex roots. When the velocity v is such that (13.37) has complex roots, these represent oscillatory solutions which imply negative populations and such waves are physically unrealistic. The bifurcation value for v, v_c say, between realistic and unrealistic solutions is the value when (13.37) has a double root as in Figure 13.8(c). Thus the range of allowable wavespeeds of travelling waves is determined by v_c. This is given by setting $f = 0$ and $df/d\lambda = 0$ and eliminating λ to get an equation for v_c in terms of the parameters. After considerably more algebra we find that, to first-order in ε and δ, v_c is given by the positive real roots of $g(v_c^2)$, where $g(z)$ is given by

$$\begin{aligned} g(z) = &\left[4\mu + (d-\mu)^2\right] z^3 + 2\left[3\mu(1-d)(3d+\mu) + (d+\mu)^2(2d+\mu)\right] z^2 \\ &+ \mu^2\left[(d+\mu)^2 - 6(1-d)(3d+\mu) - 27(1-d)^2\right] z \\ &- 4\mu^4(1-d). \end{aligned} \tag{13.38}$$

When the threshold criterion (13.34) holds, $g(z)$ is negative and d^2g/dz^2 is positive at $z = 0$. A rough sketch of $g(z)$ shows it has a unique positive root which corresponds to the minimum possible velocity for an epizootic wave.

We now show that it is not possible for a trajectory to go from the critical point at $s = 1, q = 0, r = 0$ to that at the origin where $s = q = r = 0$. On linearising (13.35)

about the origin we find (after more algebra) the eigensolutions

$$\begin{pmatrix} s \\ q \\ r \\ r' \end{pmatrix} = \mathbf{a}\exp\left[-\frac{(\mu+\delta)\xi}{v}\right], \quad \mathbf{b}\exp\left[\frac{v}{2} \pm \left(d+\frac{v^2}{4}\right)^{1/2}\right]\xi, \quad \mathbf{c}\exp\left[\frac{\varepsilon\xi}{v}\right],$$

where

$$\mathbf{a}^T = \left[0, \frac{d-\mu-\delta}{\mu} - (\mu+\delta)^2\mu v^2, 1, -\frac{\mu+\delta}{v}\right],$$
$$\mathbf{b}^T = \left[0, 0, 1, \frac{v}{2} \pm \left(d+\frac{v^2}{4}\right)^{1/2}\right], \quad \mathbf{c}^T = [1,0,0,0],$$

and the superscript T denotes the transpose. Sufficiently close to the origin, trajectories which approach the origin are linear combinations of the two eigensolutions with negative exponents, and so they approach the origin in the plane $s = 0$. For the system (13.35) 'time' is reversible, in the sense that we can replace ξ by $-\xi$ and trace backwards along any trajectory. Setting $\tau = -\xi$ in (13.35) and taking $s = 0$ initially, we see that $s = 0$ for all positive τ irrespective of the initial values of r and q. This implies that a trajectory which has $s = 0$ for any ξ had $s = 0$ for all previous ξ, and has $s = 0$ for all subsequent ξ. So, a trajectory cannot come from $s = 1$, enter the $s = 0$ plane, and approach the origin.

This implies that a travelling wave can only occur if there is a trajectory from $s = 1$ to the critical point (s_0, q_0, r_0) and this requires, as we expected, that condition (13.34) must hold. To determine the behaviour of the wave as it approaches this critical point, we now linearise (13.35) about (s_0, q_0, r_0) to get (after more algebra) the eigenvalues

$$\lambda_1, \lambda_2 = \frac{1}{2}\left\{v - \frac{\mu}{v} \pm \left[\left(v-\frac{\mu}{v}\right)^2 + 4(\mu+d)\right]^{1/2}\right\} \tag{13.39}$$

to first-order in ε and δ, and

$$\begin{aligned}\lambda_3, \lambda_4 = &\pm \frac{i}{v}\left[\frac{\varepsilon\mu d(1-d)}{\mu+d}\right]^{1/2} \\ &- \varepsilon d\left[2v(\mu+d)^2\right]^{-1}\left[\mu(1-d)\left(\frac{\mu}{v^2}-1\right) + (\mu+d)^2\right]\end{aligned} \tag{13.40}$$

to second-order in ε and δ. λ_1 is positive and so, near the critical point, any solution which approaches (s_0, q_0, r_0) as $\xi \to \infty$ is a linear combination of the eigensolutions corresponding to λ_2, λ_3 and λ_4. Since $|\lambda_2| \gg |\operatorname{Re}(\lambda_3, \lambda_4)|$, the amplitude of its eigensolution decays much more rapidly than that of the eigensolutions of the complex eigenvalues. Thus, sufficiently far back in the tail of the wave (that is, for sufficiently

large ξ), the solutions corresponding to the complex eigenvalues govern the behavior of the travelling wave. The eigenvectors corresponding to these eigenvalues are given by

$$\begin{pmatrix} s - s_0 \\ q - q_0 \\ r - r_0 \\ r' \end{pmatrix} = \begin{pmatrix} 1 \\ \pm i \left[\dfrac{\varepsilon d(1-d)}{\mu(\mu+d)} \right]^{1/2} \\ \pm i \left[\dfrac{\varepsilon \mu(1-d)}{d(\mu+d)} \right]^{1/2} \\ \dfrac{\varepsilon \mu(1-d)}{v(\mu+d)} \end{pmatrix}$$

which, on taking an arbitrary real linear combination of the eigensolutions, gives, for sufficiently large ξ,

$$\begin{aligned} s - s_0 &\sim [A \cos \omega\xi/v + B \sin \omega\xi/v] \exp(-\lambda\xi/v), \\ q - q_0 &\sim \frac{\omega}{\mu}[A \sin \omega\xi/v - B \cos \omega\xi/v] \exp(-\lambda\xi/v), \\ r - r_0 &\sim \frac{\omega}{d}[A \sin \omega\xi/v - B \cos \omega\xi/v] \exp(-\lambda\xi/v). \end{aligned} \tag{13.41}$$

Here ω is the period of the waves, given by the imaginary part of the complex eigenvalues divided by v, and λ is the decay rate of the amplitude, given by the real part of these eigenvalues divided by v. A and B are constants, which depend on the way the trajectory approaches (s_0, q_0, r_0), which of course cannot be determined from a linear analysis.

Let us now exploit the smallness of ε and δ to obtain certain useful asymptotic analytical approximations (Murray et al. 1986). From the approximate steady state forms (13.36) we note that the rabid fox density $r_0 = \mu q_0/d$. From (13.41) we see that far back in the tail of the wave, that is, ξ large, we also have $r - r_0 \sim \mu(q - q_0)/d$. That is, the profiles for the infected and rabid fox densities are similar, differing only in scale. In the simulations, such as those in Figures 13.9 and 13.10, of the full nonlinear system, the striking profile similarity holds for the *entire* wave. This surprising fact suggests that, in view of the complexity of the three-species model, it would be of considerable benefit if we could obtain analytically the conditions under which the travelling wave problem for the three-species model could be modelled to a high degree of approximation with a two-species model. That is, we could replace, for example, the three-species *SIR* system of susceptible, infectious, rabid populations by a two-species system of only susceptible and rabid populations. The infected, but not yet rabid, fox population is then given by a simple scaling of the rabid population, namely,

$$q(\xi) \sim \frac{dr(\xi)}{\mu}. \tag{13.42}$$

Under certain conditions it is possible to give an analytical explanation as to why this phenomenon occurs. It is not obvious from the model system (13.35). The mathemat-

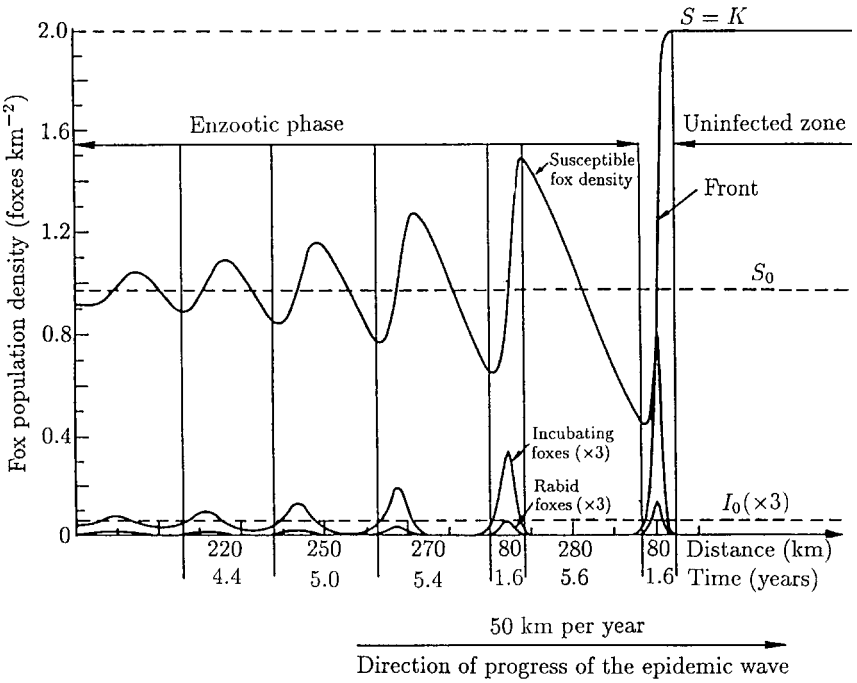

Figure 13.9. The susceptible, infected and rabid fox populations due to the passage of a rabies epidemic wave from a numerical simulation of the model mechanism (13.37)–(13.40). The fox density in the uninfected region ahead of the front of the epidemic is taken to be at a carrying capacity of 2 foxes/km^2, a typical value (averaged over the yearly cycle) for much of continental Europe. The time and distance between the recurring outbreaks and the wavespeed were obtained from the model using estimates for the field parameters given in Table 13.1 and a diffusion coefficient $D = 200$ km^2/yr. (From Murray et al. 1986)

ical analysis is based on μ being small compared with both d and the nondimensional wavespeed v, but large compared with ε and δ. The singular perturbation analysis is quite complicated and is given in detail by Murray et al. (1986).

To get the actual travelling wavefront solutions for the epizootic we must solve the partial differential equation system (13.33) numerically, starting with $s = 1$ (that is, dimensionally the susceptible population is $S = K$, the undisturbed carrying capacity) everywhere and with a small concentration of rabid foxes at the origin. When the threshold criterion (13.34) is satisfied an epidemic wave forms and travels outward from the initial concentration of rabid foxes with near constant velocity. If, of course, the threshold inequality (13.34) is violated, then rabies dies out, and the fox population returns to the carrying capacity of the environment. Figure 13.9 is an example of the travelling wavefront which evolves for parameter values appropriate to the current epizootic on continental Europe. The wave consists of the rabies front, in which the largest number of foxes die from the disease, followed by an oscillatory tail in which each successive outbreak of rabies is smaller than the preceding one. The oscillations gradually die out and the populations approach constant nonzero values with the rabid and infected fox population zero. Figure 13.10 illustrates the fluctuations in fox density for a travelling

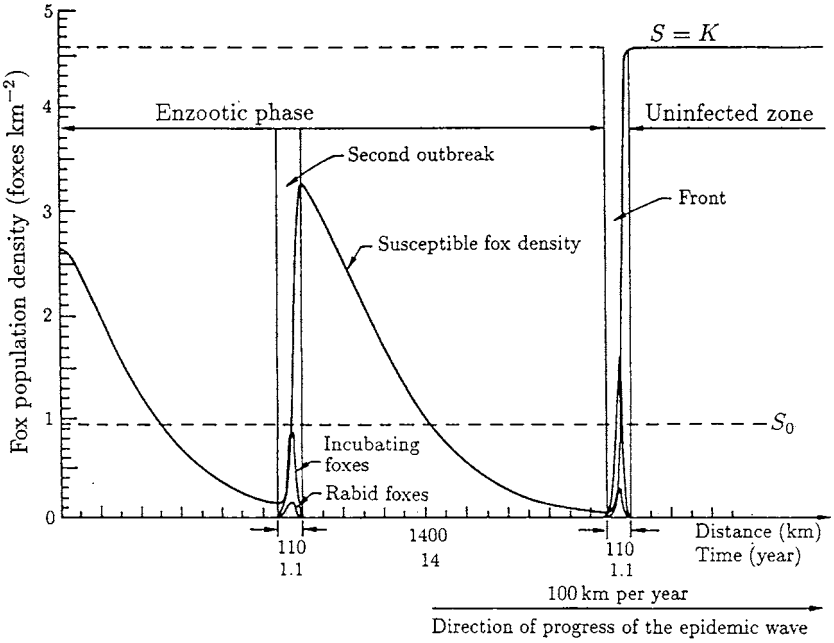

Figure 13.10. Fox populations during the passage of the rabies epidemic wave when the fox density in front of the epidemic is at the carrying capacity of 4.6 foxes/km^2, which is common in parts of England. The diffusion coefficient $D = 200$ km^2/yr, and the other parameters were taken from Table 13.1. Compare the different wavelengths and periods of the recurring epidemics following the front with those in Figure 13.9. The epidemics for England are more severe. (From Murray et al. 1986)

epizootic wave with parameters appropriate for England; note the wilder fluctuations in the susceptible population compared with those in Figure 13.9.

With the parameter values in Table 13.1, the threshold condition (13.34) is satisfied and

$$\varepsilon \quad \text{and} \quad \delta \ll 1, \quad d, \quad \mu \quad \text{and} \quad 1 - d. \tag{13.43}$$

Under these circumstances the wavefront is followed by an oscillatory tail. Analytically the minimum speed is given by $v = z^{1/2}$, where z is the unique positive root of the cubic (13.38). A contour plot for this root v is shown in Figure 13.11 for $0 \leq d \leq 1$. All of the waves found numerically appear to travel at this minimum speed which, from (13.32), is given in dimensional form as

$$V = (D\beta K)^{1/2} v. \tag{13.44}$$

For example, with the parameter values in Table 13.1, a diffusion coefficient of 200 km^2/yr and a carrying capacity of 2 foxes/km^2, we evaluate d and μ from (13.32) and then read off the appropriate v from Figure 13.11; this gives the dimensional speed of propagation as $V = 51$ km/yr.

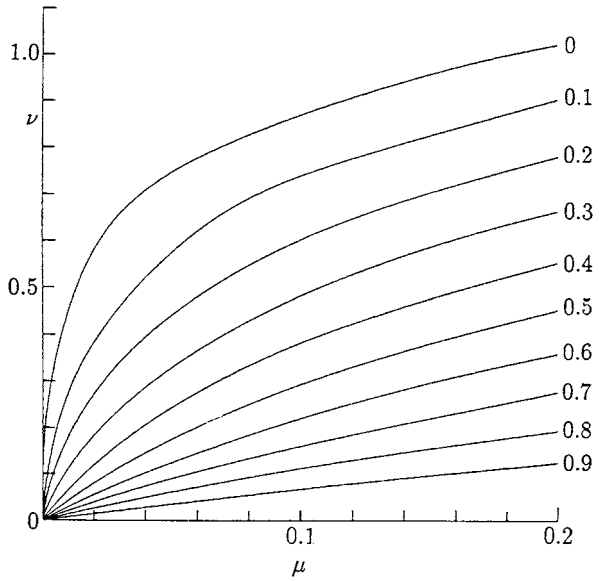

Figure 13.11. The dimensionless velocity of propagation, v, of the epidemic front as a function of the dimensionless parameter μ for various values of d. Recall that μ is related to the incubation time for the rabies virus, and d is related to the duration time of the symptomatic, infectious, stage; see (13.32). The dimensional wavespeed is given by $V = (\beta K D)^{1/2} v$. Note that $v = 0$ for $d \geq 1$, which corresponds to a carrying capacity less than the critical value. (From Murray et al. 1986).

The linear analysis near the steady state (s_0, q_0, r_0), described above, shows that for sufficiently large times the wave tends to decaying oscillations given by (13.41). In terms of the original (x, t) variables these solutions can be written in the form

$$\begin{aligned} s(x,t) &= s_0 + A\cos[\omega(t + x/v) + \psi]\exp[-\lambda(t + x/v)], \\ q(x,t) &= q_0 + \frac{1}{\mu}(s - s_0)', \\ r(x,t) &= r_0 + \frac{\mu}{d}(q - q_0), \end{aligned} \tag{13.45}$$

to first order in ε and δ, where the prime denotes differentiation with respect to $(t + x/v)$ and the nondimensional wavenumber ω is given by

$$\omega = \varepsilon^{1/2}\left[\frac{\mu d(1-d)}{\mu + d}\right]^{1/2} + O(\varepsilon^{3/2}), \tag{13.46}$$

with the decay rate λ given by

$$\lambda = \frac{\varepsilon d}{2(\mu + d)^2}\left[\mu\left(\frac{\mu}{v^2} - 1\right)(1 - d) + (\mu + d)^2\right]. \tag{13.47}$$

A and ψ are constants. Note that the oscillations in the susceptible population are 90° out of phase with both the infected and, as noted above, the rabid populations. (This symmetry is broken if the oscillations are calculated to the next order in ε and δ.) As we also noted above, the $r-q$ proportionality relationship (13.42) seems to hold universally as indicated by the numerical simulations when physically reasonable parameters are used.

The singular perturbation analysis of Murray et al. (1986) yields several useful approximations regarding the epidemic. For example, the maximum densities of infected and rabid foxes in the first outbreak, are given by

$$\begin{aligned} r_{\max} &\approx \mu \left(\ln d + \frac{1-d}{d} \right), \\ q_{\max} &\approx d \left(\ln d + \frac{1-d}{d} \right), \end{aligned} \tag{13.48}$$

which in dimensional terms are

$$\begin{aligned} R_{\max} &\approx \frac{\sigma K_T}{\alpha} \left[\ln \left(\frac{K_T}{K} \right) + \frac{K}{K_T} - 1 \right], \\ Q_{\max} &\approx K_T \left[\ln \left(\frac{K_T}{K} \right) + \frac{K}{K_T} - 1 \right]. \end{aligned} \tag{13.49}$$

Since no epidemic ensues if $K \leq K_T$, the threshold carrying capacity, both $R_{\max}$ and $Q_{\max}$ are zero for $K = K_T$. Note that both $R_{\max}$ and $Q_{\max}$ increase as K increases above K_T.

Once we have the dimensionless wavespeed $v(= z^{1/2})$ from (13.38) we can then determine the decay rate λ from (13.47). It turns out that λ is always positive. This means that the limit cycle behaviour which the diffusionless version of (13.26), that is, with $D = 0$, can exhibit for sufficiently large $K > K_T$ disappears when diffusion is taken into account: the oscillations always decay to the constant state (s_0, q_0, r_0). The dimensional decay rate is $\beta K \lambda$. The dimensional period of the recurring epidemics is

$$\tau = \frac{2\pi}{\beta K \omega},$$

where ω is given by (13.46); in terms of the original dimensional parameters, using (13.32), the period T is

$$T = 2\pi \left\{ (\alpha + \sigma + b) \left[(a-b)(\alpha+b)\sigma \left\{ 1 - \frac{\alpha+b}{\beta K} \right\} \right]^{-1} \right\}^{1/2}. \tag{13.50}$$

Note that T decreases with K. So, in general, the greater the fox density before the appearance of rabies, the less frequently rabies outbreaks will appear far behind the front; this agrees with some observations (Macdonald 1980). However, numerically it was found that close to the front, where nonlinearities are important, the time between out-

breaks may increase with K; see Figures 13.9 and 13.10. Once we have the dimensional velocity V and period T we get the dimensional wavelength $L = VT$.

Estimate for the Diffusion Coefficient D and Sensitivity of Wavespeed and Epidemic Wavelength to Variations in D

To calculate the real dimensional speed V of the epizootic, and hence the period and wavelength of the recurring epidemics which follow the main front, we need an estimate for the diffusion coefficient, which is a measure of the rate at which a rabid fox covers ground in its wanderings. Little is known about the behaviour of rabid foxes in the wild, making it very difficult to estimate D.

Andral et al. (1982) tracked three rabid adult foxes in the wild. They accomplished this by inoculating captured foxes with rabies virus, equipping them with signal-emitting collars, and releasing them at the point of capture. They traced the fox movements first during the incubation period, to determine their home ranges and normal behaviour, and then during the rabid period, to observe the changes induced by the disease. Once the foxes became rabid their pattern of daily activity changed. Drawings showing, for each fox, the incubation period range and the principal displacements during the rabid period indicate that all three left their home range at some point during the rabid phase, but none travelled very far away.

Murray et al. (1986) used the results of Andral et al. (1982) to estimate the diffusion coefficient, in a rather primitive way, from the formula

$$D \approx \frac{1}{N} \sum_{j=1}^{N} \frac{(\text{straight line distance from the start})^2}{4 \times (\text{time from the start})},$$

where the sum is over the number of all foxes involved. Using the distance between the start of the rabid period and the point of death, along with the approximate length of the rabid period, gives an estimate of 50 km^2/yr for D. Since two of the three foxes happened to die much closer to their starting position than their mean distance away from it, this is most likely a lower bound on D. An extremely rough idea of an upper bound can be gained from the maximum distance that any one fox travelled away from its starting point. About halfway through the rabid phase, one fox got as far away from its starting point as 2.7 km, giving an estimate of 330 km^2/yr as an upper bound on D.

There are other ways of estimating diffusion coefficients. For example, D can be estimated as the product of the average territory size A and the average rate k at which a rabid fox leaves home. For their two-species model, Källén et al. (1985) supposed that infected foxes leave home at the end of the incubation period of one month, that is, when they were assumed to become rabid. Taking an average territory size to be about 5 km^2, they obtained $D = 60\ \text{km}^2$. To determine D for our 3-species model, we need an estimate for the average rate at which foxes leave their territories *after* the onset of clinical disease. If N infected foxes are observed, and the jth one leaves its territory a time interval t_j after becoming rabid, then k can be estimated by

$$\frac{1}{N} \sum_{j=1}^{N} \frac{1}{t_j}.$$

Since roughly half of all infected foxes develop paralytic rabies and presumably never leave their home range, t_j is infinite for about $N/2$ foxes. For the furiously rabid foxes, if we suppose that half also never leave, and that the rest leave evenly spread out over the 6 days that the disease may take to run its course, then we can estimate

$$k \approx \frac{1}{N}\sum_{j=1}^{N/4}\frac{1}{t_j} = \frac{1}{24}\sum_{j=1}^{6}\frac{1}{j \text{ days}} = 40 \text{ yr}^{-1}.$$

Keeping the estimate of 5 km^2 for an average territory size (Toma and Andral 1977; Macdonald 1980), this gives $D = 190$ km^2/yr.

An alternative method is to estimate the mean free path and velocity of rabid foxes. The average total distance covered daily by the foxes observed by Andral et al. (1982) was 9 km during the rabid period. Suppose that this is not atypical and that, for example, a rabid fox goes 100 m at a stretch before becoming distracted and setting off in another direction. Then $D =$ (velocity) $\times$ (pathlength) gives a diffusion coefficient of 330 km^2/yr, the same as the upper bound that we estimated previously. All of these methods for estimating D should, in principle, be consistent if enough observations of rabid fox behaviour could be made. At this stage there is simply not enough known about rabid fox behaviour to get much better estimates.

Since the speed of the wave is proportional to $D^{1/2}$, changing D from 50 to 330 km^2/yr increases V by a factor of 2.6. Table 13.2 shows the sensitivity of the wavespeed and wavelength as a function of the carrying capacity for a given $D = 200$ km^2/yr.

Another difficult parameter to estimate is the disease transmission coefficient β. As we said above, this can be estimated by inverting the threshold expression (13.30). But, absolute values of fox population densities are in practice difficult to obtain; they are usually estimated from the numbers of foxes reported dead, shot or gassed, and some assumption on the percentage of the total population that this sample represents, or else by comparison of terrain with areas of known fox densities. This in turn means K_T is particularly difficult to estimate, and values of anywhere from 0.2 to 1.2 foxes/km^2 can be estimated from the values given in the literature (WHO Report 1973, Steck and

Table 13.2. Dependence of the wavespeed and asymptotic wavelength (that is, the distance between recurring outbreaks) on the carrying capacity, calculated with $D = 200$ km^2/yr and other parameter values from Table 13.1.

K (foxes/km^2) or K/K_T* Carrying Capacity	V (km/yr) Velocity of the Epidemic Front	L (km) Distance Between Successive Outbreaks/Peaks
1.5	35	150
2.0	50	210
2.5	70	220
3.0	80	250

* The parameters β and K only appear as the product βK in the calculations for the values in Tables 13.1 and 13.2. From equation (13.30), $\beta K = (K/K_T)(\sigma + a)(\alpha + a)/\sigma$, so that only a knowledge of the ratio of the actual carrying capacity to the critical value is necessary to obtain the results.

Wandeler 1980, Macdonald et al. 1981, Gurtler and Zimen 1982). Since finding K/K_T only involves comparison of population sizes, this ratio might be easier to obtain than K and K_T separately.

A relevant question at this point is how sensitive the quantitative results are to the uncertainties in the parameters. This aspect and difficulties in estimating other parameters are discussed by Murray et al. (1986).

13.6 Control Strategy Based on Wave Propagation into a Nonepidemic Region: Estimate of Width of a Rabies Barrier

We discuss here one possible control strategy as developed by Murray et al. (1986), namely, that of a possible protective barrier against the rabies epizootic which can be achieved by reducing the susceptible fox population below the critical density K_T in areas ahead of the advancing wave. This, for example, has been successful in Denmark, specifically Jutland. It has also been carried out in some regions of Italy and Switzerland, where it has been pursued with diligence, but it has had mixed results (Macdonald 1980, Westergaard 1982). Such a barrier can be created either by killing or vaccination. Since killing releases territories, there could be a more rapid colonization by young foxes which could in fact enhance the spread of the disease. Vaccination causes less disruption in the ecology, is almost certainly more effective and is also probably more economic.

For a rabies 'break' to be effective we must have reasonable estimates of both the width and the allowable susceptible fox density within it. Here we derive estimates analytically for how wide the protective break region needs to be to keep rabies from reaching the areas beyond. We also present some of the results from numerical simulations of the full equation system (13.33). In what follows, we use the term 'infected fox' to refer to all foxes with rabies, whether infectious or not.

If we observe the passage of the rabies epizootic wave at a fixed place we note that each outbreak of the disease is followed by a long quiescent period, during which very few cases of rabies occur; refer to Figures 13.9 and 13.10. The spatial and temporal dimensions are such that the secondary epidemic wave is sufficiently far behind so that the first wave will either have moved past the break, or have effectively died out by the time the second one arrives. Each successive outbreak is weaker than the previous one. So, it seems reasonable to assume that the same population reduction schemes which eradicate the first outbreak will also be effective in stopping all subsequent outbreaks from passing through. We thus only need to consider how wide the break needs to be to stop the first outbreak. The width of the break is dependent on the size of the susceptible fox population density within it.

Since we model spatial dispersal by a deterministic diffusion mechanism it is, from a strict mathematical viewpoint, not possible for the density of infected foxes to vanish anywhere. This arises from treating the fox densities as continuous in space and time, rather than dealing with individual foxes, and from using classical diffusion to model the rabid fox dispersal. Thus we cannot simply have the epizootic wave move into a break of finite width and determine whether or not the density of infected foxes remains zero on the other side; it will always be positive, although exponentially small. Thus

no matter how wide the break is, eventually enough infected foxes will in time leak through for the epizootic to start off again on the other side. Thus we must think instead of determining when the probability is acceptably small that an infected fox will reach the far side of the break.

Since the aim of any control scheme is to keep the density of foxes small, we treat the break region as one with a carrying capacity below K_T, the critical threshold value (13.30) for an epidemic, and we assume that the fox density has been reduced to this value well before the epizootic front arrives. To obtain estimates for the width of the break we investigate the behaviour of the model when the region of lowered susceptible fox density starts at $x = 0$ and extends to infinity. We first give here the results of the numerical simulations of the full system (13.33) and later in the section obtain approximate analytic results.

Figures 13.12 and 13.13 show what happens when the epizootic wave, coming in from the left, impinges on the break region. Remember that the epizootic wave cannot propagate when the carrying capacity is below the critical value K_T. Also, the point of maximum infected fox density will be at $x = 0$. As the infection wave moves into the region $x > 0$ it spreads out, decays in amplitude and the total number of infected foxes decreases. Eventually there will be less than p infected foxes/km^2 remaining, where p is some small number. Let $t_c(p)$ be the time at which this occurs. We now choose p sufficiently small that the probability of a rabid fox encountering a susceptible one after this critical time is negligible. Since the wave cannot propagate in the break region it simply decays, so, for all time the density of infected foxes is greatest at the edge of the break and decays with x, exponentially as x^2 in fact, as we show later. We choose the width of the break to be the point x_c where the infected fox density is a given (small) fraction m of the value at the origin, that is,[5]

$$I(x_c, t_c) + R(x_c, t_c) = m[I(0, t_c) + R(0, t_c)]. \tag{13.51}$$

Available evidence suggests that it has never been possible to eliminate all foxes from a region—a 70% reduction in population is about the best that can be achieved (Macdonald 1980). Figure 13.14 shows the dependence of the break width in terms of the percentage population reduction in the break, for different choices of the average duration time of clinical disease, $1/\alpha$.

In the numerical simulations for the curves in Figure 13.14, the value of βK outside the break was held at 160 yr^{-1}, the number of infected foxes at the critical time was taken to be $p = 0.5$ foxes/km^2, the ratio m in (13.51) was arbitrarily chosen to be 10^{-4} and all other parameters except α are from Table 13.1. With these assumptions, for any given choice of α, the nondimensional forms in (13.32) give $d = (\alpha + 0.5 \text{ yr}^{-1})/(160 \text{ yr}^{-1})$ and (13.30) gives a carrying capacity outside the break region of $K = 149/(\alpha + 0.5 \text{ yr}^{-1})$ foxes km^{-2} yr^{-1}. For example, if we assume that the rabid period lasts an average of 3.8 days, then $d = 0.6$ and $K = 1.5$ foxes/km^2 outside of the break. If a reduction scheme can reduce the carrying capacity to 0.4 foxes/km^2 inside the break region well before the epidemic arrives, then $s_b = 0.26$ and Figure 13.14 gives $x_b = 15$. Assuming a diffusion coefficient of 200 km^2/ yr, (13.32) gives the predicted

[5] Strictly the x_c and t_c are dimensionless here.

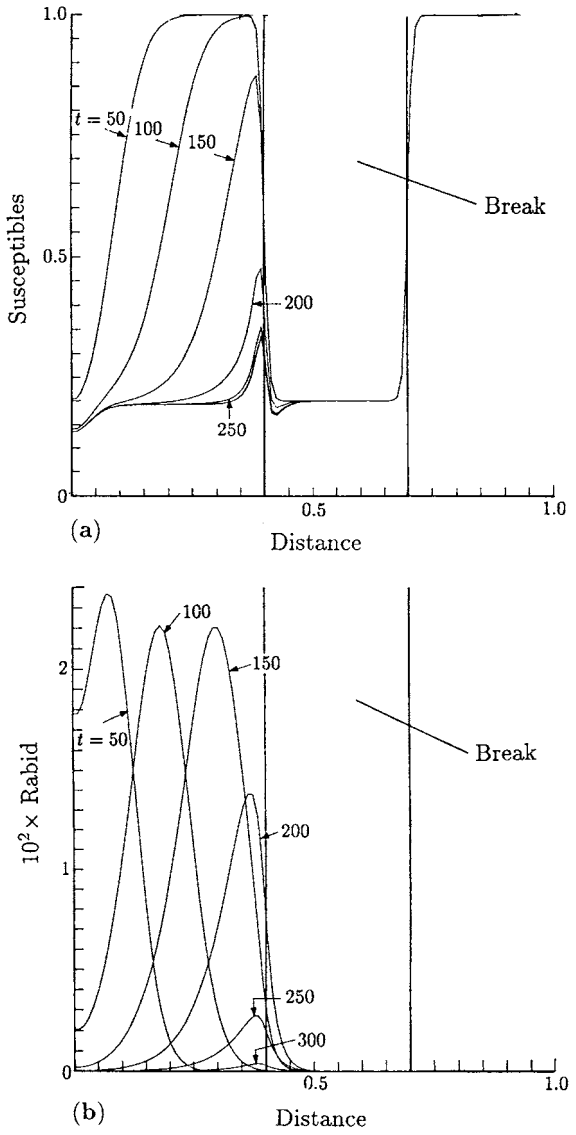

Figure 13.12. The behaviour of the travelling epizootic front when it encounters a break in the susceptible fox population. These plots show (**a**) the susceptible and (**b**) the rabid fox population densities for a sequence of times as the wave approaches the break region, stops and dissipates. They were obtained by solving equations (13.37)–(13.40) numerically with a carrying capacity of 2 foxes/km^2 in the region outside the vertical lines and of 0.4 foxes/km^2 in the region between them. Other parameter values were taken from Table 13.1. Note that the susceptible population just outside the break remains slightly higher than elsewhere, since few rabid foxes wander into this region from the right. The density of incubating foxes is proportional to the rabid population as we noted in Section 13.5: with the parameter values used, the incubating fox density is 5.6 times the rabid fox density. The times and distances are normalised values within the computer model. (From Murray et al. 1986)

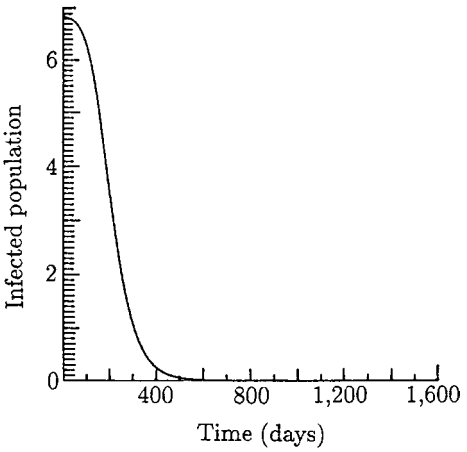

Figure 13.13. This plot shows the total infected fox density per km (the integral over x of the infected foxes $I + R$) as a function of time for the case shown in Figure 13.12 starting when the epidemic front first reaches the break. (From Murray et al. 1986)

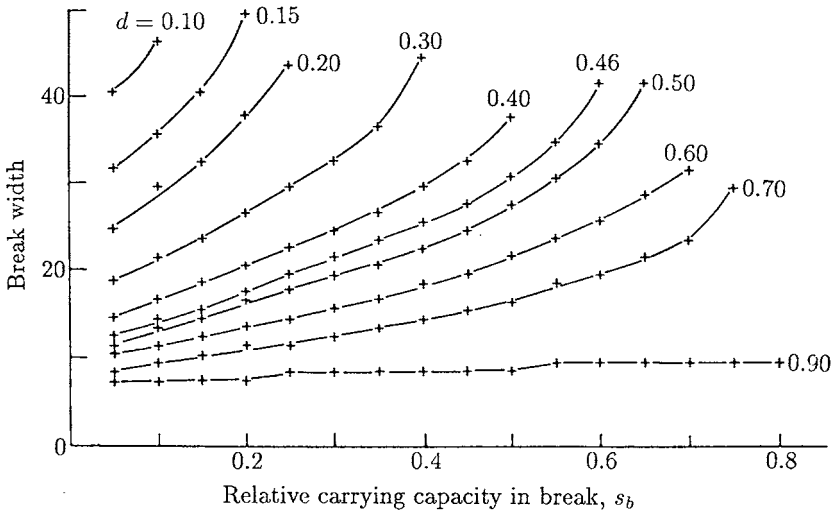

Figure 13.14. The dependence of the break width on the initial susceptible population inside the break, as predicted by the model. The break width, in nondimensional terms, is plotted against the ratio of the carrying capacity in the break to the carrying capacity outside the break for various values of the duration time of clinical disease, $1/\alpha (d \approx \alpha/\beta K)$. The curves were obtained by solving (13.33) numerically until the total infected fox population in the first outbreak is 0.5 fox/km. As described in the text, we use these curves to calculate the break width, which can be put into dimensional form using relations (13.32). The dimensional break width X_c is given by $(D/\beta K)^{1/2} x_c$, where x_c is the nondimensional break width with $m = 10^{-4}$. βK was set at 160 yr^{-1}, and all other parameters, except α, were taken from Table 13.1. For example, if we assume $1/\alpha = 5$ days then $d = 0.46$ and the carrying capacity outside the break is 2 foxes/km^2. If the carrying capacity inside the break is assumed to be 0.4 foxes/km^2 then $s_b = 0.2$ and this figure predicts $x_c = 18$. Assuming $D = 200\ \text{km}^2/\text{yr}$, the predicted break width X_c is then 20 km. (From Murray et al. 1986)

break width as 17 km. Of course, the choice of p and m depends on how cautious we want to be: Murray et al. (1986) discuss the sensitivity of the model to variations in these. The maximum value of $I + R$ at t_c for all of the calculations was less than 0.15 foxes/km^2. Even with m as large as $m = 10^{-2}$ there are fewer than 0.0015 infected foxes per square kilometre on the protected side of the break.

13.7 Analytic Approximation for the Width of the Rabies Control Break

We can determine analytically an approximate functional dependence of the break width on the parameters. The behaviour of the various fox population densities in the break region after the epizootic wave has reached it should be similar to the situation in which a concentrated localised density of infected and rabid foxes at time $t = 0$ (with the same total number of I and R as for the epizootic wave) is introduced at $x = 0$ in a domain where the carrying capacity is everywhere equal to the initial fox density in the break. We can then obtain an estimate of the break width by looking at the following idealised problem. Suppose that the carrying capacity is zero for all x, which implies that the susceptible fox density $s = 0$. At time $t = 0$, take $r = r_0\delta(x)$ and $q = q_0\delta(x)$, where $\delta(x)$ is a Dirac delta function (that is, we consider all of the r_0 rabid foxes are initially concentrated at $x = 0$).

We start by assuming that for $x \geq 0$, all of the susceptible foxes have been eliminated, for example, by immunization or killing. In our analysis here we make the added approximation that the nonlinear terms in the equations for the incubating and rabid foxes can be neglected. Since ε and δ are small parameters, this should be a reasonable approximation. A further justification for these approximations comes from the numerical computations of the break width, where it was found that the computed break width did not change if these terms were neglected. With these assumptions, equations (13.33) reduce to the linear form

$$\begin{aligned} \frac{\partial q(x,t)}{\partial t} &= -\mu q(x,t), \\ \frac{\partial r(x,t)}{\partial t} &= \mu q(x,t) - dr(x,t) + \frac{\partial^2 r(x,t)}{\partial x^2}. \end{aligned} \tag{13.52}$$

By symmetry, instead of considering the problem of a δ-function source of infected foxes at $x = 0$ and $t = 0$ which then move into the region $x \geq 0$, the initial conditions can be replaced by

$$q(x,0) = 2q_0\delta(x), \quad r(x,0) = 2r_0\delta(x) \tag{13.53}$$

and we then consider instead the region $-\infty < x < \infty$. The propagation of infected foxes into the break is described by equations (13.52) with initial conditions (13.53). The specific quantities of interest are the time t_c at which the population in the break has decayed to a given level, p, defined implicitly by the formula

$$\left(\frac{KD}{\beta}\right)^{1/2} \int_0^\infty [q(x,t_c) + r(x,t_c)]\,dx = p \tag{13.54}$$

and the break width, x_c, which, as discussed above, is given implicitly by

$$q(x_c,t_c) + r(x_c,t_c) = m[q(0,t_c) + r(0,t_c)]. \tag{13.55}$$

We first estimate t_c. Integrating equations (13.52) with respect to x from 0 to ∞, we get the two ordinary differential equations

$$\begin{aligned} \frac{dQ^*(t)}{dt} &= -\mu Q^*(t), \\ \frac{dF^*(t)}{dt} &= -dF^*(t) + dQ^*(t), \end{aligned} \tag{13.56}$$

where

$$Q^*(t) = \int_0^\infty q(x,t)\,dx, \quad F^*(t) = \int_0^\infty [q(x,t) + r(x,t)]\,dx.$$

The initial conditions for (13.56) are $F^*(0) = q_0 + r_0$, $Q^*(0) = q_0$. The first of equations (13.56) is trivially solved for $Q^*(t)$ and Q^* which is then used in the second equation to obtain the following equation for F^*, namely, the (scaled) total number of foxes present in the region $x > 0$,

$$\frac{dF^*}{dt} = -dF^* + dq_0 e^{-\mu t}. \tag{13.57}$$

With the given initial conditions, the solution to this equation is

$$F^*(t) = \left[q_0 + r_0 - \frac{dq_0}{d-\mu}\right] e^{-dt} + \frac{dq_0}{d-\mu} e^{-\mu t}. \tag{13.58}$$

The critical time t_c can then be determined from (13.54) by solving the equation

$$F^*(t_c) = p\left(\frac{\beta}{KD}\right)^{1/2}.$$

Note that each of the two terms on the right-hand side of (13.58) involves an exponential factor. Since, for reasonable values of the field parameters, $d > \mu$ and $d - \mu = o(1/t_c)$, the first of those terms can be neglected in comparison with the second if t_c is sufficiently large. Let us assume this is the case, and verify it *a posteriori*. So, neglecting the first term, the resulting algebraic equation can be solved to give

$$t_c \approx \frac{1}{\mu} \ln\left[\frac{d\left(\frac{KD}{\beta}\right)^{1/2} q_0}{p(d-\mu)}\right]. \tag{13.59}$$

Typical values for δ and μ are 0.46 and 0.08, respectively. $(KD/\beta)^{1/2}q_0$ can be approximated from Figure 13.13 and the fact that $q \approx dr/\mu$, so that the total number of infected foxes satisfies

$$\int_{-\infty}^{\infty} (I + R)\, dX = \left(\frac{KD}{\beta}\right)^{1/2} \left(1 + \frac{\mu}{d}\right) q_0.$$

From Figure 13.13,

$$\int_{-\infty}^{\infty} (I + R)\, dX \approx 6.9 \text{ foxes/km},$$

giving $(KD/\beta)^{1/2}q_0 \approx 5.9$ foxes/km. For $p = 0.5$ fox/km, (13.59) gives an estimate of $t_c \approx 33$ for these values of the parameters, and so the ratio of the two exponentials $\exp[-dt_c]$ and $\exp[-\mu t_c]$ is approximately 3×10^{-6}, which justifies neglecting the smaller exponential in (13.58) in the above analysis.

We now derive an estimate for the break width x_c. This involves solving the problem posed by (13.52) with (13.53). The first of (13.52) gives

$$q(x, t) = 2q_0\delta(x)e^{-\mu t}. \tag{13.60}$$

Substituting this into the second equation gives

$$\frac{\partial r}{\partial t} = -dr + \frac{\partial^2 r}{\partial x^2} + 2q_0\mu\delta(x)e^{-\mu t} \tag{13.61}$$

the solution of which, with initial conditions (13.53), is of the form

$$r(x, t) = \frac{2r_0}{\sqrt{\pi t}} \exp\left[-\frac{x^2}{4t} - dt\right] + e^{-\mu t} r^*(x, t),$$

where $r^*(x, t)$ is the solution of

$$\frac{\partial r^*}{\partial t} = (\mu - d)r^* + \frac{\partial^2 r^*}{\partial x^2} + 2q_0\mu\delta(x) \tag{13.62}$$

with homogeneous initial data. This equation can be solved using Laplace transforms.

Denote the Laplace transform of r^* by ρ, that is,

$$\rho(x, s) = \int_0^{\infty} r^*(x, t)e^{-st} dt, \quad \operatorname{Re} s > 0.$$

Then ρ satisfies the inhomogeneous ordinary differential equation

$$\frac{d^2\rho}{dx^2} + (\mu - d - s)\rho = -\frac{2q_0\mu\delta(x)}{s}, \quad -\infty < x < \infty, \quad \operatorname{Re} s > 0. \tag{13.63}$$

We are only interested in the solution for $x > 0$; it is given by

$$\rho(x, s) = \mu q_0 \frac{\exp[-(s + d - \mu)^{1/2} x]}{s(s + d - \mu)^{1/2}}.$$

So, inverting the transform, we get

$$r^*(x, t) = \frac{\mu q_0}{2\pi i} \int_C \frac{\exp[-(s + d - \mu)^{1/2} x] e^{st}}{s(s + d - \mu)^{1/2}} \, ds, \tag{13.64}$$

where C is the Bromwich contour. The singularities of the integrand are a pole at $s = 0$ and a branch point at $s = -(d - \mu)$. The branch cut can be taken along the negative real axis to the left of the branch point, and so the contour of integration can be deformed to lie above and below the negative real axis. Since it is only necessary to evaluate $r^*(x, t)$ for $t = t_c$, it can be assumed that $t \gg 1$ in the integral (13.64). If we now use the method of steepest descents (see, for example, Chapter 6 in the book by Murray 1984) the main contribution to the integral is given by the residue at the pole $s = 0$; the contribution from the branch cut is exponentially small in comparison, provided that

$$\left(\frac{x}{2t}\right)^2 \ll d - \mu. \tag{13.65}$$

This inequality is shown to hold below. We thus arrive at the asymptotic solution for $r(x, t)$ given by

$$r(x, t) \sim \frac{r_0}{\sqrt{\pi t}} \exp\left[-\frac{x^2}{4t} - dt\right] + \frac{\mu q_0}{\sqrt{d - \mu}} \exp\left[-\mu t - (d - \mu)^{1/2} x\right]. \tag{13.66}$$

To estimate the break width, note that the formula (13.55) cannot be directly used since, with (13.60), $q(x, t)$ always involves a δ-function. Instead, we replace (13.55) by

$$r(x_c, t_c) = m r(0, t_c). \tag{13.67}$$

The assumptions (13.65) and $t \gg 1$ can again be used to justify neglecting the first term in (13.66) as compared with the second. S_0, from (13.67) and (13.66), an estimate for the break width is given by

$$x_c \sim (d - \mu)^{1/2} \ln\left(\frac{1}{m}\right). \tag{13.68}$$

If we take $m = 10^{-4}$ together with the parameters used previously to estimate t_c, then assumption (13.65) is easily verified to be valid for $t = t_c$ and $x = x_c$ since $(x_c/2t_c)^2 \approx 0.05$ and $d - \mu \approx 0.38$.

Note that, at least to leading order, the formula for x_c is independent of the critical time t_c. The calculation of t_c was only necessary for the purpose of verifying the 't large' assumption that was made throughout the analysis.

In dimensional terms, (13.68) gives, using (13.32),

$$X_c \sim -\frac{1}{\beta K} - \left(\frac{D}{\alpha + b - \sigma}\right)^{1/2} \ln m, \tag{13.69}$$

with typical values for these parameters given in Table 13.1.

In the expression (13.68), the dependence of x_c on δ and m roughly agrees with Figure 13.14. It also suggests that the break width should not be very sensitive to p, which, as shown by Murray et al. (1986) is the case when the carrying capacity in the break is not too close to the critical value.

13.8 Two-Dimensional Epizootic Fronts and Effects of Variable Fox Densities: Quantitative Predictions for a Rabies Outbreak in England

In general fox populations are not uniform, but instead vary according to the hospitality and carrying capacity of the local environment. This is very much the case in England, where interestingly some of the highest densities (by a factor of two to three) are in cities such as Bristol.

We first present the results of what happens when the epizootic wave encounters a localised region of different carrying capacity from the surrounding environment. The model system is still (13.26) except that in this two-dimensional situation, the diffusion term in the equation for the rabid population in (13.26) is replaced by $D\nabla^2 R$. Suppose that the carrying capacity, K, and the initial susceptible fox density are equal to a uniform value everywhere on a square region, except for a small patch in the centre of the square, where they have different values. We now introduce a uniform distribution of rabid foxes along one edge of the square, so that a one-dimensional epidemic front starts off across the square, and solve the model equations numerically. Figure 13.15 shows the resulting rabid and susceptible fox population densities for the case of a higher initial susceptible density in the patch.

From Figure 13.15(b) we see that the front moves faster through the region of higher carrying capacity as we would expect heuristically. The residual fox population, once the first outbreak has moved past, is slightly lower in the pocket of higher K than in the surrounding region. The converse of these effects is obtained if the wave encounters a pocket of lower susceptible fox density. One interesting feature is that the pocket of lowered density provides a sort of protection to the region just adjoining it. There are never as many cases of rabies in a ring around the outside of this region, and the final susceptible population density is higher there than farther away. The break region of the previous section also exhibits this feature, which arises because the region of lower density does not provide as many rabid foxes to diffuse into this area—there is, in effect, a preferential direction for the diffusion. The pocket of higher density has the opposite effect. Here the epidemic moves ahead of the epidemic front into the pocket of higher density; see the central figure in Figure 13.15(c). This focusing effect could account for some of the cases when outbreaks of rabies appear in advance of the front. These effects are the likely cause of the tortuous form of the epizootic front shown in Figure 13.3.

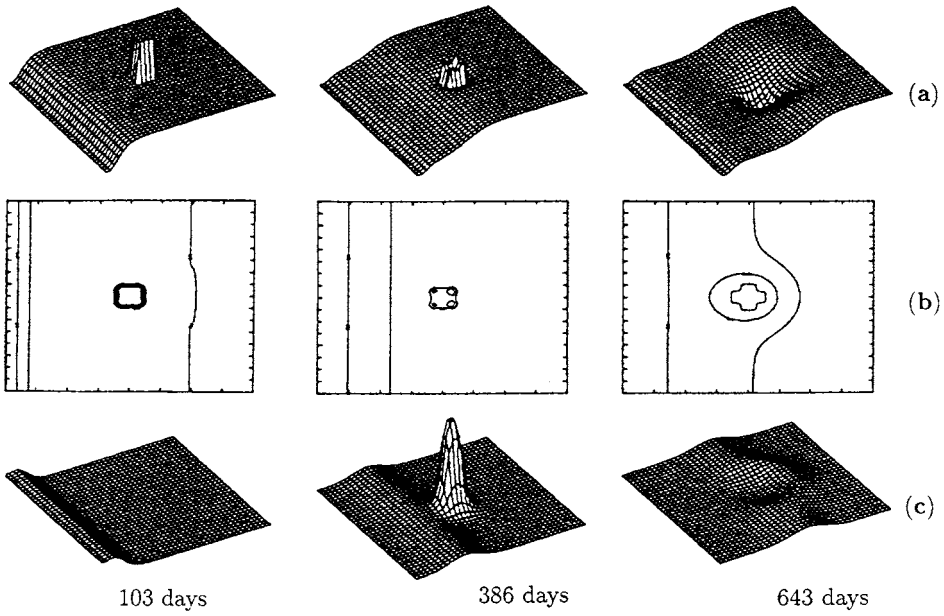

Figure 13.15. Effect on the epidemic front on encountering a pocket of higher initial susceptible fox density (and hence carrying capacity). Equations (13.37)–(13.40) were solved on a square, with the initial rabies-free fox density and the carrying capacity uniform everywhere except in a rectangular region in the centre, where they were raised by a factor of 1.7. The results are shown for a sequence of three times, namely, as the wave comes in from one side, as it passes the higher density pocket and after it passes. (**a**) Three-dimensional plot of the susceptible fox population density. (**b**) Contour plot of the susceptible fox density, with contour intervals of 0.1, where the density is normalised to have a maximum of 1. (**c**) Three-dimensional plot of the rabid fox density at each point in the square. (After Murray et al. 1986)

As mentioned before, England has remained rabies-free (except for a minor epidemic after World War I) due mainly to the strict quarantine laws[6] and high public awareness of the potential dangers. With the proximity of the disease in the north of France and the increased private boat traffic between continental Europe and Britain it seems inevitable that the disease will be brought into Britain in the near future. The appearance of rabies in Britain would be particularly serious, as we mentioned above, because of the high density of foxes, both urban and rural, in England. An additional cause for concern is the apparent compatibility of these urban foxes with cats (Macdonald 1980). If no control measures are applied, which admittedly would certainly not be the case, the epidemic would move quickly through England. We can use the model here to obtain a rough estimate for the position of the epidemic front if rabies is introduced into the fox population.

Macdonald (1980) gives a map of estimated fox densities in England (but excluding high urban pockets). Murray et al. (1986) covered the lower half of England with a grid, and assigned a density to each square based on the values given on his map. Contour

[6]In 2000 these were relaxed for selected countries if the animals had been vaccinated and underwent a series of other measures, such as blood tests and tagging, to ensure the animals are unquestionably rabies free.

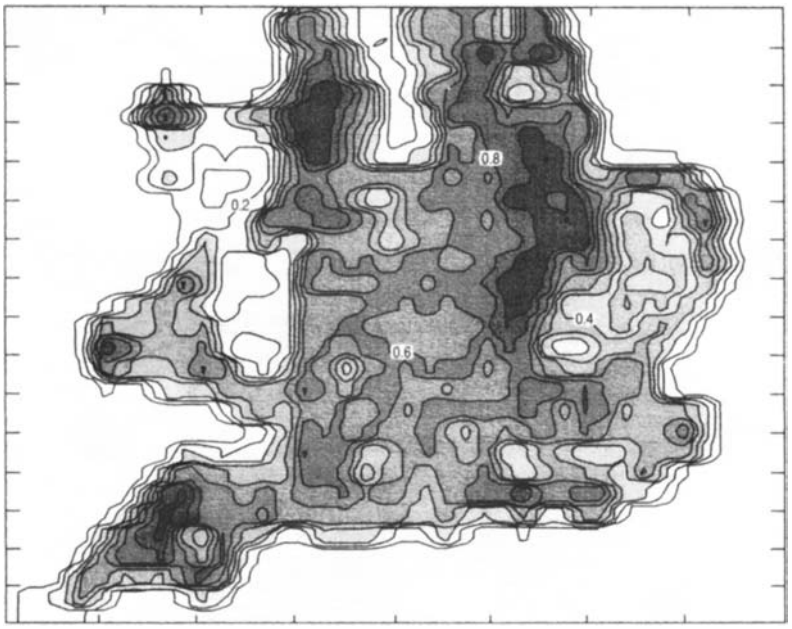

Figure 13.16. Fox densities in the southern half of England which were used in our numerical simulations. In the actual contour plots values are scaled to lie between 0 and 1, with 1 corresponding to 2.4 adult foxes/km^2 in Springtime, or to an average of 4.6 foxes/km^2 throughout the year. These values are based on Macdonald's (1980) estimates, who emphasises that the density map is probably not very accurate but is based on educated estimates. (From Murray et al. 1986)

lines of these densities, normalised from 0 to 1 were used; a shaded density map is shown in Figure 13.16. A value of 1 corresponds to 2.4 adult foxes per square kilometre in Springtime. The model studied is, in fact, in terms of fox densities averaged over the yearly cycle. Prior to the introduction of rabies, the population increases to its yearly high just after whelping, then gradually returns to the adult Springtime population. The average density is roughly the mean between the populations just before and just after whelping. The ratio of males to females is about 1.2:1, and females have an average of 3.7 to 4.2 cubs each year (Lloyd et al. 1976). Thus the average population is about 1.9 times the springtime adult population, and 1 corresponds to a carrying capacity of 4.6 foxes/km^2, the darkest shading, in Figure 13.16.

Using the carrying capacities (and initial fox densities) shown in Figure 13.16, and supposing, by way of illustration, that the rabies epidemic starts near Southampton, the two-dimensional form of (13.33) was solved numerically. The parameter values given in Table 13.1 were used, and the diffusion coefficient was taken to be 200 km^2/yr. The numerical simulations took about 120 minutes on a CRAY XMP-48 at the Los Alamos National Laboratory. The results are shown in Figures 13.17 and 13.18. The position of the front every 120 days is shown in Figure 13.17. We see that with such high fox densities the epidemic very quickly reaches most of the region studied. Within 4 years the front has effectively reached Manchester. The sequence in Figure 13.18 shows that, just as in the uniform density case, most of the cases of rabies are concentrated in a

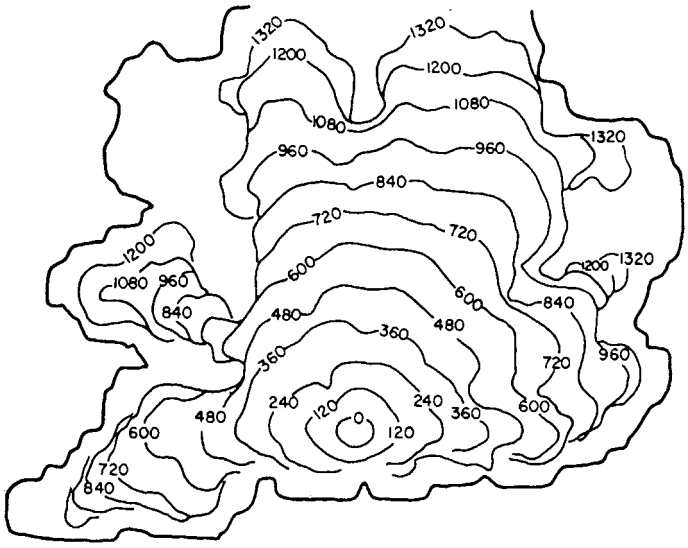

Figure 13.17. The position of the wavefront every 120 days predicted by the model (13.33) and the spatially heterogeneous fox densities in Figure 13.16; that is, some of the parameters are space-dependent. Here a diffusion coefficient of 200 km^2/yr was taken with the other parameter values from Table 13.1. (From Murray et al. 1986)

narrow band at the front; the susceptible population is effectively decimated by the epidemic and partially regenerates before another wave starts again. Figure 13.18 shows the second outbreak starting off from Southampton, about 7 years after the first one.

These quantitative predictions can, of course, only be rough estimates. Macdonald (1980) emphasises that the fox densities in his map are only educated guesses, based on his knowledge of fox ecology. As we said above, not enough is known about the behaviour of rabid foxes to obtain a sharp estimate for the diffusion coefficient, which means that the speed of the wave may be anywhere from a half to four-thirds of our calculated result. We have also neglected such geographical factors as rivers, which tend to provide a channel for the epidemic, speeding its movement parallel to the banks and temporarily halting its direct passage. However, this relatively simple *SIR*-model provides a plausible quantitative first estimate for the progression of rabies in England if an epidemic were allowed to move unchecked. The model also provides a means of estimating realistic break widths which, at the very least, would seriously impede the spread of the disease.

The model we have investigated incorporates many of the salient features of the disease and the ecology of foxes. The model is sufficiently simple to enable us to obtain fairly reliable estimates for all of the parameters except the diffusion coefficient, for which we obtained a range of possible values. Analysis of the model produces certain predictions for the behaviour of the epidemic wave, in different environments, which provides some quantitative insight into the spatial spread of the epidemic and the transmission mechanisms responsible for its spread. For example, it is not known whether the primary reason for the spatial spread of the epidemic is the encroachment of confused

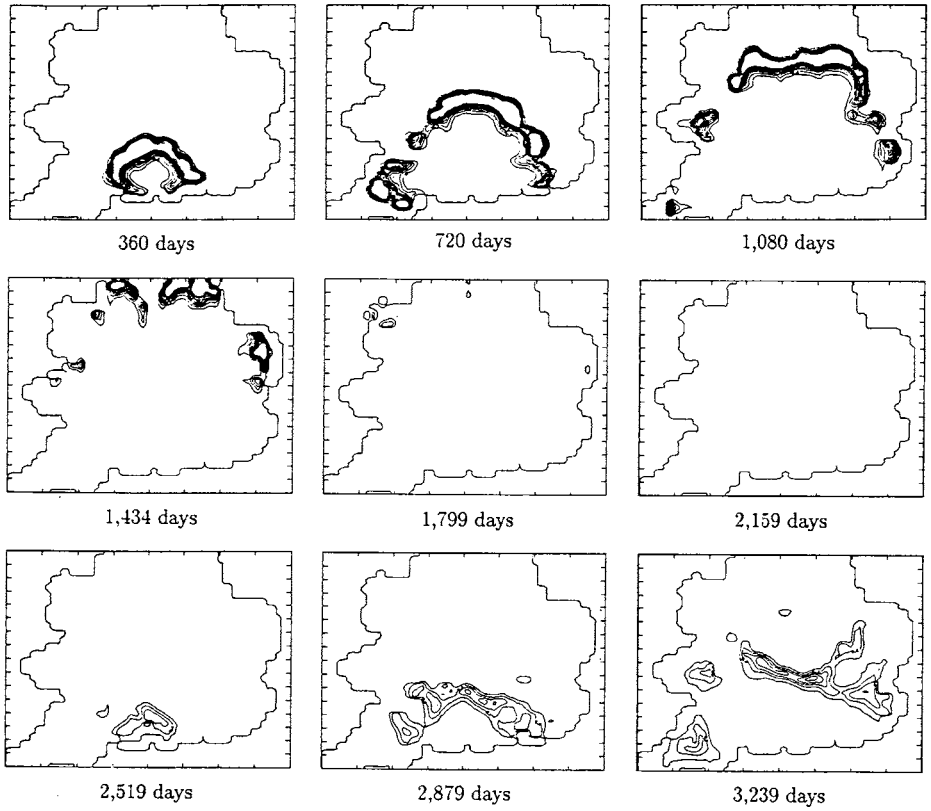

Figure 13.18. The epidemic front as it moves through the southern part of England. This was obtained by numerically solving (13.33) with the local carrying capacities and initial susceptible fox densities shown in Figure 13.16. A localised density of rabid foxes was initially introduced at Southampton on the south coast and allowed to spread. Contour plots of the rabid fox densities are given at a sequence of times, as the wave moves outward from its source. Note that, just as in the one-dimensional case, there are few rabid foxes in the region behind the front. Note also the reappearance of the second epidemic wave of lower intensity, which starts about 7 years after the initial outbreak and moves outward at the same speed. Here $D = 200\ \text{km}^2/\text{yr}$. and other parameter values are taken from Table 13.1. (From Murray et al. 1986)

rabid foxes onto their neighbour's territories, as we have assumed, or the migration of young foxes who carry the disease with them while healthy, or if both mechanisms are equally important. By isolating one of these mechanisms, we can determine how the epidemic wave behaves if that is the primary factor in its spatial spread, and compare the results with observation in continental Europe to see if it is possible for it to be the dominating factor. Our results indicate that the confused wandering of rabid foxes is sufficient to account for much of the behaviour of the current epidemic. It would be interesting to investigate a model in which migrating young foxes are the primary cause for spatial spread of rabies. It is also known that a certain percentage of foxes are immune to rabies. Such effects as these can be incorporated into the model framework here and this we investigate in the following section.

The agreement of our model with the available epidemiological evidence is quite good, despite the uncertainty in the size of the diffusion coefficient. For an initial fox density of 2 foxes/km^2, which is similar to densities reported for much of the continent, and for any reasonable choice of diffusion coefficient, the speed of the epidemic front, 25–65 km/yr, obtained from the model, encompasses the range of 30–60 km/yr usually observed. The speed of the wave increases with fox density, and drops to zero as the fox density decreases to the critical value. The model also predicts that rabies will essentially disappear for a period of about 5 years after the first outbreak, and then reappear, with the second outbreak weaker than the first. This correlates well with what has happened in many parts of Europe. Another interesting feature which emerges from the model is the enhanced movement of the rabies epidemic into regions of higher density *in advance* of the rest of the front. As we suggested, this may help to explain why outbreaks seemingly far in advance of the main epidemic occasionally occur.

It is possible for a strip of lowered susceptible fox population to check the progression of the epidemic, and protect an uninfected region ahead of the front. For this method of control to be efficiently applied, it is essential to have an indication of how wide an effective break region must be. For our model control scheme, Figure 13.14 gives nondimensional estimates for this width. If there are 2 foxes/km^2 initially, and the reduction scheme is 80% effective, then Figure 13.14 gives a break width of 10–25 km, depending on the diffusion coefficient. This is of the right order of magnitude when compared with the protective break which has proved effective in Denmark and parts of Switzerland. In Denmark, intensive control measures were applied to a strip 20-km wide with less intensive measures used in an adjoining 20-km strip.

The question of what method should be used to contain an outbreak is interesting. The model here suggests that vaccination would be more effective than gassing or poisoning since the former would help to restrict the spread of infective foxes whereas the latter would enhance the spread. It seems that chicken heads impregnated with vaccine have proved reasonably effective in Ontario: it relies on efficient scavenging by the foxes. This is not necessarily the case with urban populations[7] (personal communication from Dr. Stephen Harris, 1988). Another problem with vaccination in general is that sometimes the level of vaccination in one species may induce the disease in another as seems to be the case with the red and grey fox.

The probability that rabies will eventually reach England and other uninfected regions is not small. It is clearly of considerable importance to understand as much as possible about the disease, its transmission and how it spreads, well before it arrives. The density of foxes in England is much greater in many areas than on the continent, and the epidemic may proceed differently there. Figures 13.17 and 13.18 summarise some of the model's predictions for a particular choice of diffusion coefficient, and some estimates for the current fox populations in the southern half of England. Perhaps the most disturbing aspect of these results is the rapidity with which the epidemic would move through the central region, namely, at speeds of around 100 km/yr. No less disturbing is the reappearance of the disease several years after the passage of the epidemic front: a relatively free rabies period would certainly give rise to complacency.

[7] Interestingly the life expectancy of urban foxes is significantly less than for rural foxes—all the fast food in their 'menu du jour' no doubt.

13.9 Effect of Fox Immunity on the Spatial Spread of Rabies

It is known that a certain proportion of foxes develops a natural immunity to rabies. It is of interest to try and quantify its effect on the spatial spread of the disease. This was done by Murray and Seward (1992) and it is their modification of the models discussed in the above sections that we briefly consider here; see their paper for full details and more complete comparative results with those we obtained above. They showed that with realistic estimates for the size of the immune class, immunity has little effect on the propagation speed of the initial wave of the rabies epidemic but it does affect the behavior of the periodic outbreaks associated with the oscillating tail of the wave. They also studied the effect on the width of a rabies break which would be required to contain the epidemic and included the effect of spatial dispersal of susceptible and infected foxes. They finally investigated the hypothesis that the required break width might depend on whether the break was created by killing foxes or by vaccinating them against rabies. They found that the break width does not change significantly unless the rate of spatial dispersal is large and, of course unless the immune class increases significantly. We discuss their model since the methodology is not restricted to the spatial spread of rabies. With this in mind we also include diffusion of all species.

In the *SIR* model in the above sections we assumed that all rabid foxes die. In fact some foxes have been found to recover from rabies and a certain proportion of the survivors develop immunity to the disease. Steck and Wandeler (1980) found that about 2% of all infected red foxes in a number of experimental studies developed immunity. It is more difficult to evaluate the immune status of the fox population in the wild. Steck and Wandeler (1980) also presented data which suggest that not more than 8% of foxes living through the passage of an epidemic front are actually immunized against the disease. However, some estimates put the proportion of immune foxes as high as 20% in the U.S.A., where rabies is spread by both the grey (*Urocyon cinereoargenteus)* and the red fox. (Due to the mixture of species, our model is not directly valid in this case, although it could be extended by the appropriate choice of parameters.) Wandeler (1987) noted that the rarity of documented survival of clinical disease in experimentally and naturally infected animals is in contrast to frequent reports of rabies-neutralizing antibodies in sera collected from wild animals, and also that it is not clear whether these reports actually demonstrate survival of the clinical disease or not. Overall, it appears that the development of immunity is possible but that it has little effect on the spread of the disease. It is of interest, therefore, to investigate the effect of introducing an immune class into the model in Section 13.5. We expect that, for small values of the proportion of foxes developing immunity, the results produced by the modified model will differ little from those of the original. It is interesting to develop such a model not only for pedagogical reasons but also to confirm this belief, quantify the effect on the spatial spread as the immune class increases and the effect of immunity transfer to cubs.

We now divide the fox population into four groups: susceptible foxes, with a population density S; infected, but noninfectious, foxes, with a density I; infectious, rabid foxes, R; and immune foxes, Z. This division is again based on the long incubation period of 12–135 days that the rabies virus undergoes in the infected animal. As stated above, during this time the animal seems to behave normally and does not transmit the disease. Recall that the clinical period is a relatively short period of 1–10 days.

The key assumptions are those listed in Section 13.5, numbered (i)–(vi), together with the following.

(i) Rabies is not always fatal. Rabid foxes die at an average per capita rate α (where $1/\alpha$ is the average duration of clinical disease) and recover to develop immunity at an average per capita rate γ. Values for γ are obtained from the percentage p of rabid foxes that become immune, where

$$p = \frac{\gamma}{\alpha + \gamma}.$$

Foxes that recover without developing immunity would form only a small proportion of the susceptible class so we do not include them here.

(ii) Rabid and infected foxes continue to put pressure on the environment and die of causes other than rabies but they have a negligible number of healthy offspring.

(iii) Immune foxes may have susceptible or immune offspring. We examine the two extreme cases: either all the offspring are assumed to be susceptible or all the offspring are assumed to be immune.

These new assumptions (i)–(iii) together with those in Section 13.5 suggest the following amended model in place of (13.26).

$$\begin{aligned}
\frac{\partial S}{\partial T} &= (a-b)\left[1 - \frac{N}{K}\right] + a^* Z - \beta RS, \\
\frac{\partial I}{\partial T} &= \beta RS - \sigma I - \left[b + (a-b)\frac{N}{K}\right] I, \\
\frac{\partial R}{\partial T} &= \sigma I - \alpha R - \gamma R - \left[b + (a-b)\frac{N}{K}\right] R + D_R \frac{\partial^2 R}{\partial X^2}, \\
\frac{\partial Z}{\partial T} &= \gamma R + (a - a^*) Z - \left[b + (a-b)\frac{N}{K}\right] Z,
\end{aligned} \tag{13.70}$$

where now the total population is

$$N = S + I + R + Z.$$

If immune foxes are assumed to have only susceptible offspring then $a^* = a$; if they have only immune offspring, $a^* = 0$. We consider here only the one-dimensional problem since our primary concern is to investigate the changes in the spatial spread of rabies due to the inclusion of an immune class. In particular, we can consider the effect of including an immune class on (i) the speed of the epizootic wave, (ii) the behaviour of the recurring epidemics after the passage of the main epidemic front as shown in the above sections and (iii) control measures.

Speed of Propagation of the Rabies Epizootic

We now nondimensionalise the model system using the same dimensionless variables and parameters as in (13.29) but with the addition of one which measures immunity. For ease of reference we give these again here, namely,

$$\begin{aligned} &s = \frac{S}{K}, \quad q = \frac{I}{K}, \quad r = \frac{R}{K}, \quad z = \frac{Z}{K}, \quad n = \frac{N}{K}, \\ &\varepsilon = \frac{a-b}{\beta K}, \quad \delta = \frac{b}{\beta K}, \quad \mu = \frac{\sigma}{\beta K}, \quad d = \frac{\alpha+b}{\beta K}, \quad v = \frac{\gamma}{\beta K}, \\ &x = \left(\frac{\beta K}{D}\right)^{1/2} X, \quad t = \beta K T, \end{aligned} \tag{13.71}$$

which give

$$\begin{aligned} \frac{\partial s}{\partial t} &= \varepsilon(1-n)s + (\varepsilon+\delta)^* z - rs, \\ \frac{\partial q}{\partial t} &= rs - (\mu + \delta + \varepsilon n)q, \\ \frac{\partial r}{\partial t} &= \mu q - (v + d + \varepsilon n)r + \frac{\partial^2 r}{\partial x^2}, \\ \frac{\partial z}{\partial t} &= vr + [(\varepsilon+\delta) - (\varepsilon+\delta)^*]z - (\delta + \varepsilon n)z, \end{aligned} \tag{13.72}$$

where $n = s + q + r + z$ and $(\varepsilon+\delta)^* = (\varepsilon+\delta)$ if the immune class produce only susceptible offspring, or $(\varepsilon+\delta)^* = 0$ in the case of all immune offspring.

We wish to investigate a range of values for the percentage, p, of rabid foxes that recover and become immune. The parameter γ in the v grouping in (13.71) is given by

$$p = \frac{\gamma}{\alpha + \gamma}.$$

The other dimensional parameter values in (13.70) are given in Table 13.1 together with the diffusion coefficient $D_R = 200$ km^2 year^{-1}; recall the difficulty in estimating the diffusion coefficient.

We first consider the case in which immune foxes have susceptible offspring. The four-class model was solved numerically by Murray and Seward (1992) for five values of the percentage of immune foxes: $p = 2\%, 5\%, 10\%, 15\%, 20\%$. Although we believe the larger values are not appropriate in this model for the European situation, we include them to see the effect on the model predictions. The shapes of both the initial wave and the recurrent outbreaks were found to vary only slightly between the three-class and the four-class models: they look like the shapes in Figures 13.9 and 13.10. However, they found that the effects of introducing an immune population are:

(i) the speed of the initial wave decreases;

(ii) the levels of the infected and rabid populations are not as high in the initial outbreak;

(iii) the susceptible population is not reduced as severely when the rabies outbreak occurs;

(iv) the time between recurrent outbreaks is reduced.

The first three of these are as we would expect intuitively while the fourth point follows from them. These effects become more marked as the immune percentage increases. From the asymptotic analysis and numerical results for the three-class system in Section 13.5 the speed of the initial wave is about 51 year^{-1} when $K = 2$ fox km^{-2} and 103 km year^{-1} when $K = 4.6$ fox km^{-2}. The computed wavespeeds in the four-class cases are given in Table 13.3.

Table 13.3. Speed of the rabies epizootic front for various immunity levels and fox densities. (From Murray and Seward 1992)

$K = 2$ fox km^{-2}		$K = 4.6$ fox km^{-2}	
Immune	Wave Speed (year^{-1})	% Immune	Wave Speed (km year^{-1})
0	51	0	103
2	49	2	102
5	47	5	100
10	43	10	96
15	40	15	92
20	36	20	89

The main effect of the inclusion of the immune population (but with susceptible offspring) is in the tail of the initial wave. With the three-class model, it takes about 5 years for the susceptible fox population to recover sufficiently for a secondary outbreak of rabies to occur when $K = 2$ fox km^{-2} and 11 years when $K = 4.6$ fox km^{-2}. In the four-class case, the first recurrent outbreak occurs after a much shorter period, as shown in Table 13.4. Murray and Seward (1992) found that the susceptible population is not

Table 13.4. Time to secondary outbreak and dependence on susceptible offspring. (From Murray and Seward 1992)

$K = 2$ fox km^{-2}		$K = 4.6$ fox km^{-2}	
Immune	Time to Recover (years)	% Immune	Time to Recover (years)
0	5.0	0	11.0
2	4.8	2	7.8
5	4.3	5	5.8
10	3.8	10	4.1
15	3.2	15	3.2
20	3.0	20	2.7

reduced as much by the initial outbreak in the four-class model as in the three-class case and also that the population level builds up again much more rapidly, which accounts for the reduced time between recurrent outbreaks.

Another noticeable change found in the four-class case is the increased damping of the oscillations in the tail of the wave. In the spatially uniform situation, that is, (13.70) with $D_R = 0$, there is a nontrivial steady state defined by the (13.70) with $a^* = a$. In the three-class model, that is, (13.70) with $Z = 0$ and $\gamma = 0$, there is a critical carrying capacity K_T given in (13.30), for this nontrivial steady state (13.29) to exist; both the steady-state values and K_T were easily obtained after some elementary algebra. In the four-class model, the analytical solution is difficult to find but straightforward to estimate the steady states and critical carrying capacity, K_T, numerically. Murray and Seward (1992) found that as the immune percentage increases, the computed solution tends to its steady state value in a shorter time period.

In the case in which immune foxes have immune offspring only, the model was solved for the same values of carrying capacity K and immune percentage p as in the previous case. The assumption of immune offspring has no effect on the propagation of the initial outbreak—the wavespeeds are the same as those given in Table 13.2 as was confirmed numerically. This is to be expected since the immune population does not exist until that outbreak has passed.

Again, the main effect is seen in the tail of the initial wave and here the differences from the four-class model with susceptible offspring and the original three-class model are significant. After the passage of the initial epizootic wave, the immune foxes form a substantial proportion of the population and this has a considerable damping effect on successive outbreaks of the disease. With a carrying capacity of $K = 2$ fox km^{-2}, the time until a second outbreak occurs is larger than in the three-class model and increases as the immune percentage increases, as shown in Table 13.5. With $K = 4.6$ fox km^{-2} and 2% immune foxes, there is a second outbreak of rabies after 18 years; with 5% immune foxes, there is a second outbreak of rabies after 21 years. The graphs obtained are again very similar for all immune percentages greater than 5% when $K = 4.6$ fox km^{-2}.

These differences can be explained by considering the steady-state solution of the system (13.70) with $a^* = 0$. In this case, there is no physically realistic steady state

Table 13.5. Time to secondary outbreak with immune offspring. (From Murray and Seward 1992)

$K = 2$ fox km^{-2}	
% Immune	Time to Recover (years)
0	5.0
2	5.4
5	5.6
10	6.2
15	6.8
20	8.1

with positive values of I and R. The model requires that the rabies epidemic die out for a steady state to be attained, in which case (13.70) reduces to a logistic growth law for the remaining total fox population, $S + Z$. The steady state solution gives $S_0 + Z_0 = K$ and the relative values of S_0 and Z_0 are determined by their initial values. The time required for the system to approach the steady state depends on the carrying capacity and the percentage of immune foxes. As either K or p increases, the system tends to the steady state faster.

With either susceptible or immune offspring, we see that the use of the four-class model has little effect on the propagation of the initial rabies outbreak. The wavespeed only changes significantly if a high proportion of immune foxes is assumed. The main effect then of the four-class model is seen in the tail of the initial wave. The effect is very different depending on whether the immune foxes are assumed to have susceptible or immune offspring.

As we said, the assumption of only immune or only susceptible offspring is a simplification. Among other effects, immune and susceptible foxes will interbreed and the proportion of the offspring with immunity will depend on the relative sizes of the immune and susceptible populations. Equations for heritability could be included in the model but this would lead to a much more complicated system than either the three- or four-class models. The prediction from the model that a low rate of natural immunity (2%–5%) has little effect on the wavespeed is in agreement with the observation that a lack of immunity is one of the contributing factors to the spread of rabies among foxes (see, for example, Blancou 1988). The most significant effect at low immunity rates is the reduction of the time period before the secondary outbreak when $K = 4.6$ fox km^{-2}.

Immunity Effects of Control Measures Associated with a Rabies 'Break'

A major use of a model for the spread of an infectious disease is to assess various control strategies to contain the disease. As discussed in Section 13.6 one possible method is to introduce a rabies 'break' ahead of the initial wave. Recall that we consider a break to be a region where the susceptible fox population is reduced below the critical carrying capacity and hence will not sustain a propagating epizootic wave. The model here can again be used to estimate the required break width for a range of parameter values.

In practice, a break can be created by killing foxes—the method used in Denmark—by intensified hunting and gassing fox dens during whelping season (Wandeler 1987), or by vaccination, which has been used successfully in Switzerland (Wandeler et al. 1987). We can compare these two approaches using the model. As mentioned a potential difficulty with killing the foxes is that a reduced population density may encourage dispersal of foxes into the area, thus reducing the effectiveness of the break. This dispersal can be modelled by introducing diffusion terms for both the susceptible and infected fox populations, that is, including terms $D_S(\partial^2 S/\partial X^2)$ and $D_I(\partial^2 I/\partial X^2)$ in the first two equations of the three-class model. The effect of the diffusion terms will be to average the populations inside and outside the break. Yachi et al. (1989) investigated the three-class model with diffusion of susceptible and infected foxes, assuming the same diffusion rates for all three populations, and found that this could result in a significant increase in the speed of propagation of the epizootic. Murray and Seward (1992) con-

sidered smaller diffusion rates for the susceptible and infected foxes than for the rabid population. The vaccination approach can be modelled by setting the initial immune population Z in the four-class model to a nonzero value to represent vaccinated foxes.

We can again estimate the required break width by solving the system of equations numerically with data such that the region of lowered fox population density starts at $x = 0$ and extends to infinity. As the epizootic wave moves into the region, eventually the total number of infected foxes remaining will be less than F infected fox km^{-1}, where 'infected fox' now refers to any fox with rabies, whether infectious or not. The number F is chosen to be sufficiently small, that is, well below the critical carrying capacity for the disease. Let $t_c(F)$ be the time at which this occurs. Again the break width is chosen to be the point x_c where the infected fox density is a given (small) fraction m of the value at $x = 0$; that is (recall (13.51)),

$$q(x_c, t_c) + r(x_c, t_c) = m[q(0, t_c) + r(0, t_c)].$$

As noted there are two ways to model a region of lowered population density: by reducing the carrying capacity K or by reducing the initial susceptible fox population S. Reducing K corresponds to an ongoing programme of control, where the susceptible population is held at a lower level over some period of time, and is the approach used in Section 13.6. The dependence of the break width on the carrying capacity in the break, the parameter d and on F and m is shown in Figure 13.14 in Section 13.6.

When only the initial value of S is reduced, the situation is that of a 'one-off' attempt to create a break, rather than an ongoing control. Intuitively, this second approach seems less likely to be an effective means of stopping the spread of the epidemic wave but the computed results show similar break widths in both cases. We discuss this effect after explaining our method for computing the break widths in a little more detail: it is essentially the same as in Section 13.6.

Murray and Seward (1992) first considered the effect of dispersal of all foxes using the three-class model, that is, without an immune population. The model in this case is simply (13.70) with $Z = \gamma = 0$ but with diffusion terms for S and I, namely,

$$\begin{aligned}
\frac{\partial S}{\partial T} &= (a-b)\left(1 - \frac{N}{K}\right) S - \beta RS + D_S \frac{\partial^2 S}{\partial X^2}, \\
\frac{\partial I}{\partial T} &= \beta RS - \sigma I - \left[b + (a-b)\frac{N}{K}\right] I + D_I \frac{\partial^2 I}{\partial X^2}, \\
\frac{\partial R}{\partial T} &= \sigma I - \alpha R - \left[b + (a-b)\frac{N}{K}\right] R + D_R \frac{\partial^2 R}{\partial X^2}.
\end{aligned} \tag{13.73}$$

This is also the system considered by Yachi et al. (1989). As discussed above it is very difficult to estimate diffusion coefficients. A rough estimate can be made, following the procedure in Section 13.5, by taking the product of the average territory size and the average rate at which a fox leaves home. Using 5 km^2 as the average territory size and the birth rate of 1 fox year^{-1} as the rate of leaving home, gives $D_S = D_I = 5$ km^2 year^{-1}. This is most likely an underestimate; for example, Garnerin et al. (1986) estimated a limit of 8 km on the dispersion distance of young foxes, based on a discrete model for

the spread of rabies. Numerical results have been computed for values 5 km^2 $year^{-1}$, 20 km^2 $year^{-1}$, 50 km^2 $year^{-1}$ and, for interest, 200 km^2 $year^{-1}$.

We need to extend the scheme in Section 13.6 for calculating break widths to model dispersal from a region of normal population density into a break. Murray and Seward (1992) recalculated the break widths without diffusion using the method of Section 13.6 taking $F = 0.5$ fox km^{-1} and $m = 10^{-4}$. Given these values for break width, they then set up their problem data so that a break of the calculated width occurs between two regions of normal population and let the model run to observe the epizootic wave flowing into the break. Of course, as discussed above, due to the diffusion, rabies will eventually appear across the break but this will take much longer than when the break is not present. They then evaluated two control scenarios with $K = 2$ fox km^{-2}, namely, a 'one-off' approach in which the susceptible population in the break was reduced and the other in which the carrying capacity in the break was kept low, that is, an ongoing control. The break widths were similar in both cases; in fact, with diffusion coefficients $D_S = D_I = 200$ km^2 $year^{-1}$, it is apparently more effective simply to reduce the initial susceptible population. The two strategies are equally effective in that the epizootic wave takes approximately the same time to cross the break regardless of the approach used to create it. The integration time over which the results were computed corresponds to a physical time of about one year and the break is set up approximately three months ahead of the time the wave reaches it. If the 'one-off' approach were used farther in advance of the impact of the epizootic wave, it would be less effective. Also, under the 'one-off' approach, it was not possible to reduce the total infected fox population to $F = 0.5$ fox km^{-1} when the susceptible population in the break was 1.2 fox km^{-2}. Numerous graphs of the various break scenarios for various diffusion coefficients and carrying capacities are given in Murray and Seward (1992).

By way of illustration of the effects of vaccination we consider the effect of vaccination by using the four-class model with the immune population Z representing vaccinated foxes. In this case, the break width is estimated using the basic scheme in Section 13.6. We solved the model equations for propagation of the wave into a region of reduced susceptible fox density $S(X, 0)$ but with an initial population of vaccinated foxes, $Z(X, 0) = K - S(X, 0)$. If we assume that these vaccinated foxes have susceptible offspring, then the break has essentially been created by the 'one-off' approach. Vaccination is applied only once to the initial population. By letting the vaccinated foxes have 'immune' offspring, we can roughly model the effect of an ongoing vaccination programme.

Results are shown in Figure 13.19 which compares the basic break widths (that is, no diffusion, no natural immunity) from the three-class model and the four-class model when $K = 2$ fox km^{-2}. We see that the break widths from the four-class model are generally larger. The case in which the vaccinated foxes have susceptible offspring is similar to having susceptible foxes diffusing into the break. As shown in Figure 13.20, with diffusion rates in the three-class model between 20 and 50 km^2 $year^{-1}$, the break widths are similar to those from the four-class model. It is less clear why the ongoing vaccination programme is not as effective as killing the foxes. As we commented above, in the four-class model, the infected and rabid populations are not as high in the initial outbreak. However, it seems that these populations then drop off more slowly in this case than in the three-class model. As a result, it takes longer for the total infected

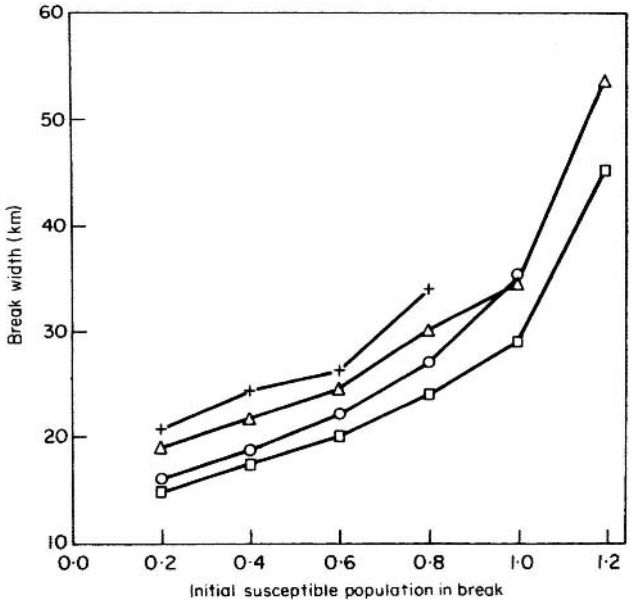

Figure 13.19. A comparison of break widths predicted by the three-class model (killing the foxes to create a break) and the four-class model (vaccination used to create the break) for a carrying capacity of $K = 2$ fox km^{-2} outside the break. Here the break width (in kilometres) is plotted against the susceptible fox population in the break, for both the ongoing control programme and the 'one-off' approach. These are for the most basic case, that is, only rabid fox diffusion in the three-class case and no natural immunity in the four-class model. The nomenclature is: □: three-class ongoing control, ○: three-class, one-off control, △: four-class, ongoing control, +: four-class, one-off control. (From Murray and Seward 1992)

fox population to drop below F, the disease spreads a little farther even in the reduced susceptible population and the calculated break width is larger. It is difficult to judge how much of this apparent spread is due to the nature of the differential equations and how much is actually due to the effect of the immune foxes on the environment. We note that there are two advantages of an ongoing vaccination programme over a 'one-off' approach—the break widths are slightly smaller and, probably more importantly, it is possible to create a break at higher population densities.

When $K = 4.6$ fox km^{-2}, it is more difficult to create a break. In the case in which vaccinated foxes have susceptible offspring, a break could not be created above a susceptible population density of 0.4 fox km^{-2}. Assuming 'immune' offspring, the break width when the reduced population density is 1.38 fox km^{-2} and $F = 1.5$ fox km^{-1} is 36 km. It was not possible to create a break using $F = 0.5$ km^{-1} at this population density.

If naturally immune foxes are included in the four-class model, the break widths decrease but the change is small if a small percentage (2–5%) is used. At 20% natural immunity, assuming either susceptible or 'immune' offspring, the breaks are 5–10 km narrower. The results are shown in Figure 13.20 for the case of 'immune' offspring (ongoing control programme).

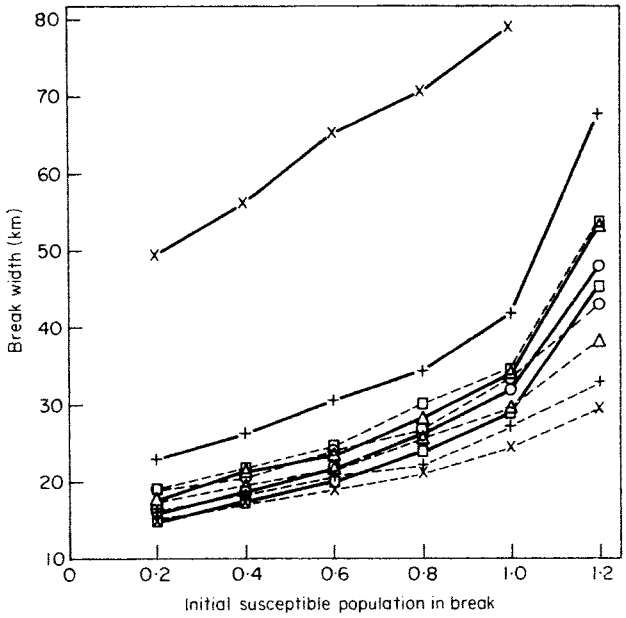

Figure 13.20. A comparison of break widths from the three-class model with varying diffusion rates (solid lines) to those from the four-class model subject to varying rates of natural immunity (dashed lines). The break width, in kilometres, is plotted against the initial susceptible fox population in the break. The carrying capacity outside the break is $K = 2$ fox km^{-2}. In both cases the break was formed by an ongoing control programme, that is, by reducing the carrying capacity in the three-class model and by assuming immune offspring in the four-class model. We see that the breaks become wider with increasing diffusion in the three-class model. In the four-class model, the break widths decrease with increasing natural immunity, more or less as we would expect. Nomenclature: □: no diffusion or immunity, ○: 5 km^2 year^{-1} or 5%, △: 20 km^2 year^{-1} or 10%, +: 50 km^2 year^{-1} or 15%, ×: 200 km^2 year^{-1} or 20%. (From Murray and Seward 1992)

Keeping in mind that these mathematical models yield only rough estimates for required break widths, we make the following observations. The most effective strategy for creating a break is to carry out a programme of culling foxes. Only if this leads to a significant dispersal of neighboring foxes into the break will it be more effective to use a program of vaccination. It is difficult to create a break in a region with a large carrying capacity. An ongoing program of control generally yields slightly smaller break widths and the possibility of creating a break at a higher fox population density than a 'one-off' attempt to create a break.

We have been primarily concerned here with the spatial propagation of an epidemic. There are important and interesting problems associated with control strategies when rabies, for example, is already in a community. An interesting and very practical model to deal with this situation was proposed by Frerichs and Prawda (1975) to deal with an urban area in Colombia: the model they proposed was for canine rabies. We discussed a modified application of their approach in Chapter 10, Volume I, when discussing control strategies for bovine tuberculosis and the interaction of cattle with badgers, which provide a reservoir of the disease.

The type of models we have discussed in this chapter have wider applicability, such as to the spatial spread of pests, killer bees (see Taylor 1977 for data on the South American spread), animals, plants and so on.

Some Caveats

What is clear from the study of these kinds of models for the spatial spread of an epidemic is that although they are quite complicated we still have had to make some major assumptions. The whole question of a break brings up the discussion in Section 13.6 on what we mean by extinction of a population in a break. That discussion is just as relevant with the modelling in this section.

Although these continuous models have helped our understanding of the transmission and spatial dynamics of disease and have resulted in some useful qualitative and often quantitative predictions, many justified criticisms can be levelled at them. For example, Mollison (1991) makes some pertinent points regarding deterministic continuous versus stochastic models. Even the (relatively) simple models we have discussed here would become orders of magnitude more difficult if we included stochasticity. In many cases the distinction between the two approaches is being able to do something or nothing with the situation under investigation; a study of the effect of stochasticity would clearly be illuminating.

It can reasonably be argued that discrete models can be made more realistic (although parameter estimation is more difficult). Also foxes live in family groups with distinct territories and so infection is more likely to spread within the whole family. Reproduction is discrete rather than continuous and so on with other aspects of fox behaviour. Such effects could be included in continuous space and discrete time models.

In all modelling there is always a trade-off between simplicity and the ability to estimate parameters and inclusion of more aspects with the diminishing ability to estimate parameters and evaluate and interpret what is predicted in the solutions. One obvious defect is the problem of a reservoir of the disease behind an outbreak wave when the calculated population is essentially at the level of extinction of the infected population; this is a problem with discrete models as well. Another related problem is the assumption that there is a mean incubation time $(1/\sigma)$ whereas in practice it is a distributed incubation time which can vary quite widely. There have been cases with dogs in quarantine in England that developed rabies even after 6 months, albeit very rarely. These last two points are clearly interrelated. Recently, in an interesting paper, Fowler (2000) has revisited the model discussed here in Section 13.6 and investigated these two aspects, namely incubation and extinction, and showed that inclusion of a distributed incubation time can explain why extinction does not occur. He further obtained asymptotic estimates for the minimum infected fox density. So, although there is obvious stochasticity in the field even extinction can be incorporated in a continuous model.

Exercises

1. Consider the dimensionless form of the epidemic model

$$S_t = -IS + S_{xx}, \quad I_t = IS - \lambda I + I_{xx},$$

where $\lambda > 0$ and look for travelling wave solutions $S(z)$ and $I(z)$, with $z = x - ct$, such that

$$S'(-\infty) = 0, \quad S(\infty) = 1, \quad I(-\infty) = I(\infty) = 0,$$

where prime denotes differentiation with respect to z.

Prove that, for all finite z, $0 < S < 1$ by showing that $S'(z) > 0$ is monotonic for all $-\infty < z < \infty$. Show also that $(S + I)' > 0$ and hence that for all $-\infty < z < \infty$, $S(z) + I(z) < 1$.

Prove that

$$\int_{-\infty}^{\infty} I(z')\,dz' > \int_{-\infty}^{\infty} I(z')S(z')\,dz' = \lambda \int_{-\infty}^{\infty} I(z')\,dz'$$

and hence deduce that the threshold criterion for a travelling epidemic wave solution to exist is $\lambda < 1$.

2. A rabies model which includes a logistic growth for the susceptibles S and diffusive dispersal for the infectives is

$$\frac{\partial S}{\partial t} = -rIS + bS\left(1 - \frac{S}{S_0}\right), \quad \frac{\partial I}{\partial t} = rIS - aI + D\frac{\partial^2 I}{\partial x^2},$$

where r, b, a, D and S_0 are positive constant parameters. Nondimensionalise the system to give

$$u_t = u_{xx} + uv - \lambda u, \quad v_t = -uv + bv(1 - v),$$

where u relates to I and v to S. Look for travelling wave solutions with $u > 0$ and $v > 0$ and hence show, by linearising far ahead of a wavefront where $v \to 1$ and $u \to 0$, that a wave may exist if $\lambda < 1$ and if so the minimum wavespeed is $2(1 - \lambda)^{1/2}$. What is the steady state far behind the wave?

14. Wolf Territoriality, Wolf–Deer Interaction and Survival

14.1 Introduction and Wolf Ecology

Territoriality is a fundamental aspect in the ecology of many mammals, particularly predatory animals such as wolves, lions, hyenas, African wild dogs and badgers, and it has been widely studied. In the case of wolves, whose prey are mainly moose and deer, an immediate question arises as to how the predator and prey coexist if the land is divided up into predator territories.[1] This in turn leads to the question of how territories are determined and maintained. It is clearly important in the ecology of such predatory animals. In this chapter we consider the question of mammalian territory formation, specifically as it applies to wolves, and its role in wolf–deer survival for which there is a considerable amount of data. In spite of the numerous studies on how pack territories are formed and maintained it was not addressed mechanistically until the mid-1990's with the mathematical modelling work of Lewis and Murray (1993), White (1995), White et al. (1996a,b), Lewis et al. (1997, 1998), Moorcroft et al. (1999) and Lewis and Moorcroft (2001) who studied the spatiotemporal effects on territory formation, territory maintenance and wolf–deer survival. Most of the material we describe in detail in this chapter is based on their work. First we give some background ecology on wolves.

The book (which has many beautiful photographs) by Mech (1991), who has studied wolves for nearly 40 years, is the best general introduction to the biology and ecology of wolves. It gives an excellent overview of the major aspects of wolf behaviour and social organisation; he also discusses some practical aspects of wolf conservation. Through his work, Mech has done much to change the often held traditional (erroneous) view of these splendid animals. He also points out that the stories of wolves attacking humans are mainly myths. He notes 'I have no doubt that if a single wolf—let alone a pack—wanted to kill someone, it could do so without trouble. When I have watched wolves close-up killing prey, they were swift and silent. A few good bites, and a human would be dead. The fact remains, however, that there is no record of an unprovoked, non-rabid wolf in North America seriously injuring a person.'

[1] I first became intrigued by this question during a visit to the University of British Columbia in the late 1970's when, over dinner, in a discussion on animal intelligence it was mentioned how particularly clever and intelligent wolves are, as has been noted regularly since at least Roman times. In Canada their main food source is often the moose. I started to wonder how, if wolves are so clever, did the moose manage to survive. It was not until the early 1990's that Mark Lewis and I started to look at the question from a mathematical modelling point of view being joined soon afterwards by Jane White.